

Source apportionment and the role of meteorological conditions in the assessment of air pollution exposure due to urban emissions

Klaus Schäfer¹, Michael Elsasser^{2,5}, Jose M. Arteaga-Salas^{2,6}, Jianwei Gu³, Mike Pitz^{3,*}, Jürgen Schnelle-Kreis^{2,6}, Josef Cyrys³, Stefan Emeis¹, Andre S.H. Prevot⁴, Ralf Zimmermann^{2,5,6}

[1] Karlsruhe Institute of Technology (KIT), Institute of Meteorology and Climate Research, Department of Atmospheric Environmental Research (IMK-IFU), Garmisch-Partenkirchen, Germany; email: klaus.schaefer@kit.edu

[2] Helmholtz Zentrum München, German Research Centre for Environmental Health (HMGU), Joint Mass Spectrometry Centre, Cooperation group „Comprehensive Molecular Analytics“, Neuherberg, Germany

[3] Helmholtz Zentrum München, German Research Center for Environmental Health (HMGU), Institutes of Epidemiology I and II (EPI), Neuherberg, Germany

[4] Paul Scherrer Institute (PSI), Gasphase and Aerosol Chemistry Group, Villigen, Switzerland

[5] University of Rostock, Institute of Chemistry, Chair of Analytical Chemistry, Joint Mass Spectrometry Center, Rostock, Germany

[6] HICE – Helmholtz Virtual Institute of Complex Molecular Systems in Environmental Health - Aerosols and Health, www.hice-vi.eu

*now with: Bavarian Environment Agency, Augsburg, Germany

Correspondence to: K. Schäfer (klaus.schaefer@kit.edu)

Abstract

As particulate matter (PM) impacts human health, knowledge about its composition, exposure and source apportionment is required. A study of the urban atmosphere assessment of air pollution exposure in the case of Augsburg, Germany, during winter (31 January - 12 March 2010) is thus presented here. Investigations were performed on the basis of particle size distributions (PSD) (5 modes, 5 positive matrix factorization (PMF) factors), aerosol mass spectrometry (3 non-refractory components, 3 PMF factors) and further air pollutants (7 gases and VOC, BC, PM₁₀, PM_{2.5}) and meteorological measurements, including mixing layer height (MLH), with one-hourly temporal resolution. Organic matter was separated by source apportionment of PM₁ with positive matrix factorization (PMF) in three factors: OOA – oxygenated organic aerosol (secondary organic factor), HOA – hydrocarbon-like organic aerosol (traffic factor or primary organic factor) and WCOA – wood combustion organic aerosol (wood combustion factor), which extend the information from black carbon (BC) measurements. PMF was also applied to the particle size distribution (PSD) data of PM_{2.5} to determine different source profiles and we assigned them to the particle sources: nucleation aerosol, fresh traffic aerosol, aged traffic aerosol, stationary combustion aerosol and secondary aerosol. Ten different temporal phases were identified on the basis of weather characteristics and aerosol composition and used for correlations of all air pollutants and meteorological parameters. The topic of meteorological influences upon nearly all air pollutants with high temporal

resolved data is studied in a comprehensive view for the first one. The high temporal resolution enabled to differentiate the relevant processes as emissions, transport and mixing as well as solar heating which are of different temporal variation during the day.

While sSource apportionment from both organic PM composition and PSD agree and show that the main emission sources of PM exposure are road traffic as well as stationary and wood combustion, But the values of the secondary aerosol factor concentrations are very often the highest ones.

The dData material were as assigned to sorted in 10 temporal phases to apply tThe hierarchical clustering analysis with the Ward method of cross-correlations of each air pollutant and PM component and of the correlations of each pollutant with all meteorological parameters. This provided two clusters: "secondary pollutants compounds of PM₁ and fine particles" and "primary pollutants (including CO and benzene) and accumulation mode particles". It was found generally that wind speed (negative), wind direction, MLH (negative) and relative humidity (positive) influence primary pollutants and accumulation mode particle concentrations. Temperature (negative), absolute humidity (negative) and also relative humidity (positive) are were relevant for secondary compounds of PM and fine particle concentrations. During a short-term phase of "wet" snow fall with strong PMC (particle mass concentration) increase the clustering provides different results than for the other 9 phases. The dominant meteorological influences on pollutant concentrations are wind speed and mixing layer height which are coupled with a certain wind direction. The compounds of the cluster "secondary pollutants and fine particles" show a negative correlation with absolute humidity, i.e., low concentrations during high absolute humidity and vice versa. The PM₁₀ limit value exceedances originated not only from the emissions but also in combination with specific meteorological conditions. NC3-10 (number concentration of nNucleation mode particles) and NC10-30 (Aitken mode particles), i.e., ultrafine particles and the fresh traffic aerosol, are were only weakly dependent on meteorological parameters and thus are were driven by emissions. The results of this case study on the basis of hourly-mean data and thus daily variations provide more information about chemical composition and causes of PM exposure during winter time in urban air pollution. implications for the sensitivity of PM compounds and gaseous air pollutants to meteorological parameters and as a consequence to a change of climate.

1 Introduction

Particulate matter (PM) and especially ultrafine particles (UFP, diameter <100 nm) are of a high health risk (Rückerl et al., 2011) as particles of smallest diameter penetrate deepest into the lungs, contribute to reduced lung function (Wu et al., 2013) and are then transported to the organs via the bloodstream. It is important from the point of view of health protection to know not only the chemical composition and emission sources, but also the meteorological influences upon the particle number concentration (PNC), particle mass concentration (PMC), different particle size fractions as well as the particle composition.

Urban regions are frequently influenced by enhanced air pollution and limit value exceedances of PM₁₀ (particles with aerodynamic diameters smaller than 10 µm, 24-hour average PM₁₀ of 50 µg/m³ should not to be exceeded more than 35 times in any calendar year) and NO₂ (hourly limit value of 200 µg/m³ should not to be exceeded more than 18 times in any calendar year) according to Directive 2008/50/EC (2008). Limit value exceedances are mainly due to emissions and chemical transformation processes, as well as meteorological influences. Wind speed, wind direction and mixing layer height (MLH) are important factors which influence exchange processes of ground level

emissions such as the abundance of gaseous pollutants (e.g., CO and NO_x concentrations) as well as PM₁₀ and particle size distributions (PSD) (Schäfer et al., 2006, 2011, 2012; Alfoldi et al., 2007; Barmpadimos et al., 2011, 2012). If the MLH is located near the ground, air pollution can be high due to a strongly limited air-mass dilution (Emeis and Schäfer, 2006). Further, temperature and humidity influence secondary gas and particle formation and particle hygroscopic growth (see e.g. Malm and Day (2001)) and thus indirectly influence air pollutant concentrations, including limit value exceedances.

An important study of wintertime aerosol chemical composition and source apportionment of the organic fraction was performed in 2010 in the metropolitan area of Paris (Crippa et al., 2013). It was found that the dominant primary sources are traffic, biomass burning and cooking. The secondary organic aerosol contributes more than 50 % to the total organic mass and includes a highly oxidized factor which is related to diverse sources including wood burning emissions. While it was concluded that particulate pollution in Paris is dominated by regional factors, direct meteorological influences were not discussed in detail.

Here, source apportionment and the role of meteorological conditions (wind, temperature, relative humidity, absolute humidity and MLH) will be discussed to get a deeper understanding of processes directing PMC, PNC and thus PSD (transport and dilution) as well as secondary particle formation and thus particle composition in the urban area of Augsburg, Germany. The main focus is on organic and ionic PM composition and its relations. This speciation of non-refractory particle composition is investigated on the basis of data from Elsasser et al. (2012).

Particle hygroscopic growth and secondary particle formation is believed to be dependent on relative humidity (Malm and Day, 2001; Yue et al., 2009; Wen et al., 2010, Zhang et al., 2010; Zhao et al., 2011; Donateo et al., 2012; El-Metwally et al., 2013; Liu et al., 2013; Wu et al., 2013, Ji et al., 2014). As the gas-phase chemistry is influenced by absolute humidity (Malm and Day, 2001; Liu et al. 2013), it will also be considered along with relative humidity. An investigation of both relative and absolute humidity is performed here required, since they are temperature dependent in a different way, and performed here.

~~Remote sensing can be applied to monitor MLH using lidar or mini-lidar like ceilometers, Sound Detection and Ranging (SODAR) and Radio Acoustic Sounding Systems (RASS). Further, this study of meteorological influences~~ focuses on the influences of MLH as monitored by remote sensing with ceilometers and Radio Acoustic Sounding System (RASS) (see Schäfer et al., 2006; Helmis et al., 2012). In the case of Augsburg, the MLH is much lower in winter (often below 500 m) than in summer (often 1500 to 2300 m) as shown by Emeis et al. (2012). During winter, the MLH mostly determines the near-surface concentration of gaseous air pollutants and PSD by up to 50 % in areas that are not influenced by strong emissions and during time periods without strong vertical mixing and advection (Schäfer et al., 2006). But also near major traffic roads air pollutant concentrations including PM₁₀ are influenced by MLH, namely the maximum concentrations (Wagner, 2014).

In this study it is hypothesised first that the MLH and other meteorological parameters also influence PM compound concentration and PSD. That is why a highly polluted winter episode in 2010, with many limit values exceedances, is analysed here using a nearly complete range of parameters (only the elemental compounds and isotopic speciation are missing).

~~The speciation of non-refractory particle composition is investigated on the basis of data from Elsasser et al. (2012). The hourly data of air pollutant and PM component concentrations and weather situations during this episode are used to characterize different temporal phases. Results of~~

~~Source apportionment and with organic molecular markers from PM composition from Elsasser et al. (2012) are applied to characterize the emission sources which cause reduced air quality/high air pollution and limit value exceedances during winter. All data on an hourly mean basis are applied. High temporal resolution (one hour) is selected to study the local as well as the regional scale and thus to find out the reasons for PM₁₀ limit value exceedances, variations of particle size distribution and chemical PM characteristics as well as air pollutant concentrations to determine the weather influences on air pollution by~~

It is hypothesised second that such a basis of one-hourly mean data provides the possibility to differentiate the relevant processes as emissions, transport and mixing as well as solar heating which are of different temporal variation during the day. Several correlation analyses of the experimental data are applied for this task and the role of dilution and transport (wind speed), mixing volume (MLH), particle growth (humidity), and secondary particle formation (temperature, humidity) will be shown quantitatively.

~~It is the objective of this case study to characterize the temporal variation of PM composition during a severe winter pollution episode in an urban area, to define the sources of such an episode and the role of meteorological conditions in PM inorganic and organic components and gaseous pollutants exposure and in the strength of different sources of such an episode. The high concentrations and limit value exceedances as well as their potential human health impact will be explained.~~

2 Measurement methods and data

2.1 Study area

The measurements were performed in Augsburg, Germany, a town with 268,000 inhabitants in 2010 (Stat. Jahrbuch, 2013), and situated in a rural area at the river Lech. The Lech flows northbound perpendicular to the Alps (about 100 km south of Augsburg) towards the Danube in a shallow valley about 10 km wide and 100 m deep. Under synoptically calm conditions with weak pressure gradients, we observe light winds from the South at night and from the North to the Northeast during the day. For stronger large-scale pressure gradients, the winds do not deviate much from the large-scale synoptic winds (Jacobbeit, 1986). The prevailing wind direction in such cases is from the Southwest where there are no big emission sources near Augsburg. A number of measurement sites were operated and are described below.

2.2 Urban background site in the city

The measurement site for the determination of particle characteristics was located on the campus of the Augsburg University of Applied Sciences / Hochschule Augsburg (HSA) which is approximately 1 km to the Southeast of the city centre. Within a radius of 100 m, it is surrounded by campus buildings, a tram depot and a small company. The nearest main roads are to the Northeast at a distance of 120 m and a larger main road with crossing this main road is to the Southeast at a distance of 270 m. Within a radius of approximately 200 m, the monitoring site is almost completely surrounded by university and residential areas, apart from a small park located in to the Northwest. HSA was carefully selected as an urban background site by taking into account the representativeness of a single monitoring station for the exposure of the general population to UFP (Cyrus et al., 2008).

The PM composition was measured continuously by an aerosol mass spectrometer in the PM_1 range and by an aethalometer, which measured the BC (black carbon) content of $PM_{2.5}$. The aerosol mass spectrometer analysis determined the non-refractory particle components nitrate (NO_3^-), sulphate (SO_4^{2-}), ammonium (NH_4^+), chloride (Cl^-) and organic matter. The latter was separated by source apportionment using positive matrix factorization (PMF, see section 3.5) in three factors: OOA - oxygenated organic aerosol (secondary organic factor), HOA - hydrocarbon-like organic aerosol (traffic factor or primary organic factor) and WCOA - wood combustion organic aerosol (wood combustion factor). A high-resolution time-of-flight aerosol mass spectrometer (Aerodyne Research Inc., Billerica, MA, USA; described in DeCarlo et al., 2006) was used with a collection efficiency of 0.5 for the aerosol mass spectrometry measurements. Additionally, the fragmentation table (Allan et al., 2004) of the aerosol mass spectrometer data analysis tools (SQUIRREL v1.49 and PIKA v.1.08, Sueper, 2010) were modified according to the fragmentation table suggested by Aiken et al. (2008). These measurements and data are described in detail in Elsasser et al. (2012).

PSD were measured by a custom-built particle size spectrometer consisting of twin cylindrical type differential mobility particle sizers, from which PNC in the different size ranges 3-10 (NC3-10), 10-30 (NC10-30), 30-50 (NC30-50), 50-100 (NC50-100), 100-500 nm (NC100-500) were determined. The general set-up of this instrument has been described in detail elsewhere (Birmili et al., 1999). Size-segregated PMC were calculated from PSD data, assuming a spherical shape of particles and a mean particle density of 1.5 g cm^{-3} (Pitz et al., 2008). PM_{10} and $PM_{2.5}$ concentrations were measured by two Tapered Element Oscillating Microbalance / Filter Dynamics Measurement Systems (TEOM Model 1400a, Thermo Fisher Scientific Inc, Franklin, MA, USA). Source apportionment on the basis of PMF is performed with these data also.

The ceilometer CL31 from Vaisala GmbH, Hamburg, Germany, operated at this station, is an eye-safe commercial mini-lidar system operated at this station (Münkel, 2007; Münkel et al., 2012).

Ceilometers, that were originally developed to monitor the cloud height, are easy to handle and do not influence the surroundings by sound or light. In the absence of low clouds and precipitation and during scattered clouds, ceilometers can estimate MLH fairly well. Special software for these ceilometers provides routine retrievals of up to 5 lifted layers from vertical profiles (vertical gradient) of laser backscatter density data (Emeis et al., 2007). The ceilometers are able to detect convective layer depths exceeding 2000 m and nocturnal stable layers down to 50 m. The aerosol structures seen in the lower layers by the ceilometer agree well with the profiles of relative humidity and virtual potential temperature measured by radiosonde and derived MLH (location of strong height gradient of aerosol backscatter density and relative humidity as well as temperature inversion) as shown by Emeis et al. (2006, 2008). The radiosonde data from the station Oberschleissheim at the northern edge of Munich (about 50 km away from Augsburg) are used for comparison. Radiosonde data does not provide sufficient information as launches only occur twice daily.

2.3 Air quality monitoring network (LÜB)

The air pollution data from four stations in Augsburg of the Bavarian air quality monitoring system / Lufthygienisches Landesüberwachungssystem Bayern (LÜB) were investigated: Bourgesplatz (urban background), Karlstrasse (urban traffic site), Königsplatz (urban traffic site), and LfU (urban edge background at the southern edge of the city) (www.lfu.bayern.de/luft/index.htm#a0101). The measured concentrations include PM_{10} and $PM_{2.5}$ by β -absorption (FH62-IR, ESM-Anderson Instruments GmbH, Erlangen, Germany), CO by IR-absorption (APMA-360, Horiba, Leichlingen,

Germany), NO and NO₂ by chemiluminescence (APNA-370, Horiba, Leichlingen, Germany), O₃ by UV-absorption (APOA-370, Horiba, Leichlingen, Germany) as well as benzene, toluene and o-xylene by gaschromatography (GC-U102 BTX, Siemens, Karlsruhe, Germany) measurements.

2.4 Rural background site at the airport Augsburg

Temperature, pressure, relative humidity, wind speed, wind direction, cloud cover, precipitation and sunshine are provided by Germany's National Meteorological Service / Deutscher Wetterdienst (DWD) (Weather Request and Distribution System www.dwd.de/webwerdis). The measurement station is at the Airport Augsburg (Augsburg-Mühlhausen) about 2 km north from the ~~northern~~ edge of Augsburg.

2.5 Urban ~~edge~~-background site at the northern edge of the city

This site is at the area of the waste treatment plant / Abfallverwertungsanlage Augsburg (AVA) which is located at the northern edge of Augsburg in an industrial area near to the highway A8 and about 2 km south of Augsburg Airport (~~urban edge background site~~). PM₁₀, NO, NO₂ and O₃ were measured at this site using the same methods described in section 2.3 and CO is detected precisely by fluorescence measurements (AL5001, Aerolaser GmbH, Garmisch-Partenkirchen, Germany).

The vertical profiles of wind, dispersion parameters and temperature up to 500 m are continuously measured during stable or neutral atmospheric conditions by a RASS from Metek GmbH, Elmshorn, Germany to determine MLH. MLH by RASS is determined from the inversion of the temperature profile. For well-mixed conditions during the afternoon hours, information for determination of the MLH is unavailable. The temperature measurements agree well with the aerosol structures seen in the lower layers by the ceilometer. These characteristics of ceilometers and RASS for the automatic and continuous observation of MLH are summarized in Emeis et al. (2004), Emeis et al. (2009) and Emeis et al. (2012). In this study, MLH data from ceilometer measurements at the urban background site are taken if no RASS results are available. Further, ceilometer MLH results are used if the MLH is lower than the cloud lower boundary and if no fog is detected. If this is not the case, the available RASS data are used.

3 Analysis methods

3.1 Selection of analyses period

A one year time series of hourly-mean values of PM_{2.5} concentration measurements at the urban background site HSA from 01 October 2009 to 30 September 2010 is shown in Figure 1. The higher concentration level during winter and the PM_{2.5} concentration peaks (110.7 µg/m³ maximum on 11 February 2010) are clearly visible. Further, twelve limit value exceedances of PM₁₀ with daily mean concentrations up to 96 µg/m³ at the urban ~~edge~~-background site, LfU, were detected during winter (no NO₂ limit value exceedances). High PM_{2.5} concentrations during winter and the large number of PM₁₀ limit value exceedances motivate the study of the period from 31 January, 00:00 CET to 12 March 2010, 24:00 CET (eight limit value exceedances are during this period) in more detail.

3.2 Comparison of measurement results at different sites

As the chemical characterization of PM was measured without gaseous pollutants at the urban background site HSA, it was necessary to take data for all gaseous pollutants from another urban background site. The hourly-mean values of measurement results at the urban background sites Bourgesplatz (LÜB), LfU (LÜB), urban background site (HSA) and urban edge background site (AVA) were used since similar temporal variations were found there (see Table 1 as well as Figure S1).

The location of Bourgesplatz is very similar to the urban background-site HSA so that NO and NO_x were used from this site (higher NO and NO_x concentrations than at AVA and LfU). Unfortunately, the other pollutants are not measured here so that the CO, O₃, benzene, toluene and o-xylene concentrations were taken from the urban edge background-site LfU (higher CO and O₃ concentrations than at the site AVA). PM_{2.5} and PM₁₀ concentrations were used from the urban background-site HSA where all the other particle parameters were measured.

3.3 Definition of different temporal phases

As also done by Birmili et al. (2009) and Crippa et al. (2013), different temporal phases were defined on the basis of hourly-mean, relatively constant values of

- PMC levels (PM₁, PM_{2.5}, PM₁₀)
- Concentrations of organic and inorganic PM components and their relations
- Different PMF factors determined in aerosol mass spectrometer data analysis
- Weather characteristics (precipitation, i.e. wet deposition, wind direction, wind speed and MLH, i.e. air mass transport and dilution, temperature as well as relative humidity and absolute humidity, i.e. secondary aerosol formation conditions).

These criteria allowed the definition of 10 temporal phases (see Figure 2 and 3 as well as Figure S1 and S3). The phases are characterized by composition and meteorological parameters (quantitatively also) in Table S1 in the supplements. During the whole study period, the total variations in the concentrations of PM₁, PM_{2.5} and PM₁₀ as well as the chemical PM₁ components are-were one order of magnitude, temperatures are-ranged from -12 to +13°C and wind speeds are from 0 to 14 m/s.

3.4 Correlations of all-air pollutants and meteorological parameters

To assess the role of meteorological conditions in the air pollution exposure due to urban emissions Pearson correlation coefficients were calculated between all pollutants and of each pollutant with all meteorological parameters (including the PMF analyses results, see section 3.5) using the standardized data (see also Wen et al. (2010) and Wu et al (2013)) on the basis of hourly-mean values during the period from 31 January, 00:00 CET to 12 March 2010, 24:00 CET (984 data points).

The correlation coefficient values are given in Tables S2 and S3 in the supplements. SO₂ concentrations are-were not considered because the concentrations are normally near the detection limit of the instruments.

The correlation coefficients were then clustered using a hierarchical clustering analysis with the Ward method (Ward, 1963). Heatmaps, including a dendrogram on the columns and rows, help distinguish the results. Clusters between rows (columns) can be identified by reading the dendrogram from right to left (bottom to top). The length of the branches at each clade represents the similarity between cluster members (e.g., the longer the branch, the greater the difference). The correlation calculations also include the p-value for each correlation. The hypothesis test to obtain the p-values is testing if any correlation exists at all.

Wind polar plots were used where the wind direction is expressed as polar coordinates (circles) and the wind speed by colours. The magnitude is given in the horizontal and vertical axis and corresponds to the standardized values for each pollutant (“standardized” means that all pollutants are forced to have average = 0 and standard deviation = 1 for their data series). The comparisons between pollutants become possible by standardizing the data since this removes the effects of different measuring scales.

3.5 Comparison of Positive Matrix Factorization (PMF) analyses results

PMF is a bilinear unmixing model which provides the opportunity to describe e.g. the measured organic fraction/matter by the aerosol mass spectrometer as a linear combination of factors. A factor contains a constant mass spectrum (factor profile) and a variable contribution with time (factor strength). The factors represent physically positive concentrations. Normally, these factors are dominated by sources. A detailed description of the PMF model and analysis can be found in the studies of Lanz et al. (2007), Ulbrich et al. (2009), and Paatero et al. (1994, 1997). The PMF analysis followed the procedure described by Ulbrich et al. (2009) and is discussed in detail for this data in Elsasser et al. (2012). The PMF analysis obtained a three-factor solution performed by FPEAK 0.2 with 14285 time points and 268 mass-to-charge ratios (m/z) from m/z = 12 to 300. Normally, these factors are dominated by sources. In this three-factor solution, factors are found related to freshly emitted HOA, which is related to traffic, and WCOA. Additionally, one non-source related factor could be calculated for OOA, which is mainly of secondary origin.

The PMF method was also applied in Augsburg to the PSD data to identify possible particle sources by (Gu et al., (2011). In this study, five different source profile factors were determined and assigned to the following particle sources, given the corresponding maximum size for PNC / PMC in the brackets: nucleation (8 nm / -), fresh traffic (20 nm / -), aged traffic (40 nm / 200 nm), stationary combustion (80 nm / 300 nm) and, secondary aerosol (350 nm / 500 nm), long-range dust (/ 2000 nm) and re-suspended dust (/ 4000 nm). However, we utilized PSD data covering 64 size bins ranging from 3.8 nm to 8.8 μ m as input data. Since no measurement error was available for PSD, the uncertainties were calculated according to empirical equations (see described in Gu et al., (2011)). In our study, only PSD data in the size range from 3.8 nm to 800 nm were available for the time period, which is studied here, as the Aerodynamic Particle Sizer (Model 3321, TSI, Shoreview, MN, US) was not in operation due to maintenance and consequently data in the size ranges 850 nm - 10 μ m and the factors long-range dust and re-suspended dust are missing.

The PMF analyses results of both data sets, described elsewhere (Elsasser et al., 2012; Gu et al., 2011), are used and compared here.

4 Results

4.1 Temporal variations

The temporal variation of concentrations of some PM-chemical fractions F factors (HOA, WCOA, and OOA and fresh aerosol), and CO, NC3-10 and NC10-30 together with the meteorological parameters (temperature, absolute humidity, relative humidity, wind speed and MLH) during the measurement campaign is shown in Figure 3. The wind speed (dilution and transport), humidity (particle growing growth) and MLH (mixing volume) show a significant influence upon the concentration of

these compounds: low concentrations during high wind speeds / high MLHs / low relative humidity / high absolute humidity and high concentrations during low wind speeds / low MLHs / high relative humidity / low absolute humidity. ~~Rain or snow occurred in all phases during certain time spans except phase 1.~~ In contrast, the concentrations of NC3-10 (number concentrations of nucleation mode particles which are defined in the size range 3 nm – 10 nm), NC10-30 (number concentrations of Aitken mode particles which are defined in the size range 10 nm – 100 nm) and fresh traffic aerosol are only weakly dependent on meteorological parameters. This is also shown by all Pearson correlation coefficients in Tables S2 and S3 ~~in the supplements~~.

4.2 Cross-correlations of each air pollutant and PM component

High CO as well as NO_x and benzene concentrations are indicators of heavy air pollution. CO and benzene concentrations are correlated strongly with HOA, soot (BC) and NC100-500, i.e. accumulation mode particles which are formed in the atmosphere and defined in the size range 100 nm – 1 µm (see Figure 4 as well as all Pearson correlation coefficients in ~~the supplements~~ Table S2 ~~during the total measurement period and Figure S2 for each measurement period~~). Figure 4 shows a heatmap of the Pearson cross-correlations between all air pollutants (correlations equal to 1 are coloured in white), including dendograms for rows and columns (obtained with hierarchical clustering). This presentation is “diagonally symmetric” in that what is shown on the top-diagonal is the same as in the low-diagonal. There are no strong correlations of NO, NO₂ or NO_x with NO₃⁻. O₃ shows negative correlations with all pollutants, sometimes ~~low~~^{higher} than -0.5 as with CO, benzene, NO₂, HOA, BC and NC100-500. Significant positive correlations between the pollutants (see Table S2 also) are found within these clusters:

- a) PM_{2.5}, PM₁₀, NO₃⁻, SO₄²⁻, NH₄⁺, OOA, WCOA, secondary aerosol, WCOA, and stationary combustion aerosol, PM_{2.5}, and PM₁₀, i.e. secondary pollutants-PM compound and fine particle concentrations, as well as
- b) CO, benzene, BC, HOA, BC and NC100-500, i.e. primary pollutants and accumulation mode particle concentrations.

There seems to be a third cluster containing NO, NO₂, NO_x, o-xylene, toluene, aged traffic aerosol NC30-50 and NC50-100 but the correlations are mostly lower than 0.8. Nucleation aerosol, fresh traffic aerosol, NC3-10 and NC10-30 are also correlated. This clustering also suggests that there are similar temporal variations of the pollutants in each of the two clusters.

4.3 Correlations of pollutants with meteorological parameters

The results of hierarchical clustering of correlations between pollutants and meteorological parameters during the measurement period (each temporal phase and total period) are shown in Figure 5 including the dendrogram on the columns and rows. Due to the positive correlation of absolute humidity and temperature, there is a similar negative correlation of OOA, secondary aerosol, NO₃⁻, SO₄²⁻, NH₄⁺, PM_{2.5}, PM₁₀ and stationary combustion aerosol (cluster “secondary pollutants-PM compounds and fine particles”) and NC100-500 with temperature and absolute humidity. Other pollutants are nearly independent from absolute humidity (see Figure 6 also).

Phase 4 shows opposite relations in comparison to all other phases as mentioned in section 3.3 and will be discussed later (section 4.4). The Ozone-O₃ correlations are of different sign in comparison to all the other correlations shown in Figures 4 and 5.

We observe the following significant correlations (p -value < 0.05) between pollutants and meteorological parameters (see all Pearson correlation coefficients in Table S3 in the supplements also):

- Significant correlations with all meteorological parameters for NO_3^- , SO_4^{2-} , and NH_4^+ , OOA, HOA, WCOA, NO_2 , benzene, o-xylene, $\text{PM}_{2.5}$, PM_{10} , NC30-50, NC50-100, NC100-500, aged traffic, secondary aerosol and stationary combustion aerosol i.e. the secondary pollutants mainly (except HOA, benzene, o-xylene).
- Significant correlations with relative humidity, absolute humidity, wind speed and MLH (but not with temperature) for NO, NO_x and toluene.
- Significant correlations with temperature, relative humidity, wind speed and MLH (but not with absolute humidity) for BC, CO, NC3-10, i.e. nucleation mode particles, and nucleation aerosol, i.e. primary pollutants.
- Significant correlations with relative humidity, wind speed and MLH (but not with temperature and absolute humidity) for NC10-30, i.e. Aitken mode particles.
- Significant correlation with wind speed only for fresh traffic aerosol.

In Figure 5, showing the intercorrelations between pollutants and meteorological parameters in the different phases, the dendrogram on the columns shows a clustering of the phases. It is difficult to conclude from this dendrogram general groups for the correlations of air pollutant concentrations with the meteorological parameters. If one is looking for a grouping as a first step, the dendrograms show that phase 4, the phase with highest PM pollution during the investigated period, is a special case and cannot be included in a group. Otherwise, three groups of phases can be identified from the correlations with single meteorological parameters, which are shown in Figure 6 together with phase 4 and the total measurement period, and can be characterised as follows:

1. Very low PMC (PM_1 , $\text{PM}_{2.5}$, PM_{10}) with high organic content in PM_1 . Some peak CO, NO and NO_x concentrations. Highest temperatures (up to $+13^\circ\text{C}$). Highest wind speeds (up to 14 m/s). Wind directions from west-southwest to south-southeast. Phases 1, 2, and 7.
2. High PMC (PM_1 , $\text{PM}_{2.5}$, PM_{10}) with higher organic and SO_4^{2-} content as well as high NO_3^- content in PM_1 concentration peaks. Highest CO, NO and NO_x concentrations. Temperatures mostly below 0°C , down to -12°C . Lowest wind speeds (below 7 m/s). All wind directions. Phases 5, 6, and 10.
3. Low to mean PMC (PM_1 , $\text{PM}_{2.5}$, PM_{10}) with higher NO_3^- content in PM_1 . Some peak CO, NO and NO_x concentrations. Temperatures from -12 up to $+7^\circ\text{C}$. Wind speeds between 1 and 11 m/s. Wind directions around north (from west-southwest to east). Phases 3, 8, and 9.

These groups, formed from similarities between certain phases, are different in PM composition and concentrations, CO, NO and NO_x concentrations, temperature, wind speed and wind direction. In phase 4, continuous snowfall occurred and is not considered to be typical. Otherwise, the O_3 correlations are similar within the three groups.

The dependencies of concentrations on wind direction and wind speed are shown in the plots of Figure 7. Maximum concentrations are/were found during wind directions from the Southeast, which are/were characterised by low wind speeds (often wind speed < 1 m/s), for "Primary pollutants" (shown for CO and HOA in Figure 7) and NO, NO_2 , NO_x , o-xylene, toluene, NC30-50, and NC50-100, i.e. the Aitken mode particles. There is no wind direction dependence for "Secondary pollutants PM compounds" and NC3-10, i.e. the nucleation mode particles, and NC10-30. Wind speeds lower than 3 m/s during the events of high concentrations correspond with a low MLH (see Figure 3). As the compounds are/were measured at different sites, it can be concluded that wind speed and MLH influence the concentrations of primary pollutants, in addition to local emission sources.

These findings agree well with the results published by Wen et al. (2010) and Wu et al (2013) as well as the statement by Tai et al. (2010) and Tandon et al. (2010) that up to 50 % of the particulate variability can be explained with temperature, relative humidity, precipitation, and circulation (wind and MLH). But different temporal resolutions of data are used for these studies: Wen et al. (2010) daily variations, Tandon et al. (2010) 8 h mean values as well as Wu et al. (2013) and Tai et al. (2010) daily mean values.

The comparison of temporal variations of the pollutants during the total measurement period found that a shift in the concentrations of the pollutants by one or two hours against the meteorological parameters provides higher correlation coefficients and very similar temporal variations. This means that after a change in the weather characteristics, the concentrations of pollutants follow within one to two hours of this weather change (see also Tandon et al. (2010)).

4.4 Special phase characterised by continuous snow fall

Quantitative analyses of the pronounced phase 4 (see Figure 5) are discussed in detail here. Phase 4 (one-day-event with strongest PMC increase during “wet” snow fall) is also shown in Figure 6 since it ~~is~~was not included in the ~~a group of phases as defined in~~ ~~cluster analyses for grouping (see section 4.3).~~ Wind speed is lowest during the observation period which is a main influence leading to high concentrations of locally emitted air pollutants. Wind speeds ~~are~~were from 0.5 to 5 m/s and wind directions ~~are~~were from west-northwest and north-northwest. Temperatures ~~are~~were from -9 to -4°C.

During this event, higher WCOA, OOA, HOA and SO_4^{2-} contents as well as high CO, NO and NO_x concentrations existed. These are implications for a relatively high contribution of wood combustion emissions in the surrounding residential areas due to these uncomfortable weather conditions. The correlations between all pollutants (see Figure 8) are higher than the mean (see Figure 4 and ~~in the supplements~~ Table S2, except NO_3^- and NH_4^+), implying nearly all pollutants show this strong concentration increase. The clustering provides a different result than for the other phases: a cluster including Aitken and accumulation mode particles (NC30-50, NC50-100 and NC100-500), aged traffic aerosol, NO_3^- and NH_4^+ with low correlations and no strong concentration increase as well as a cluster with all local and regional compounds (benzene, OOA, WCOA, o-xylene, HOA, toluene, BC, secondary aerosol, CO, PM_{10} , $\text{PM}_{2.5}$ including SO_4^{2-} , nucleation aerosol, NC3-10, fresh traffic aerosol, NC10-30, NO_x , NO and NO_2) with lower correlations.

High positive correlations of all pollutants (except NO_3^-) with temperature, wind speed, MLH (all these correlations are normally negative) and relative humidity were found. The positive correlations most probably are caused by the short time span of this phase (one day only), i.e. the diurnal variation of temperature, wind speed and MLH which is in agreement with the concentration increase.

4.5 Positive matrix factorization (PMF) comparison

The source apportionment by PMF from PSD data and from PM_1 composition provides different factors which can address similar sources. Further, these factors show different temporal variation. The factor secondary aerosol from PMF analyses of PSD data (see also mass concentrations in Figure S23) ~~is the~~showed maximum values during the time periods 05 – 20 February 2010 and on 12 March

2010. The nucleation aerosol factor is highly variable during the study period and smallest in mass concentration. The factor fresh traffic aerosol and the factor aged traffic aerosol, which is higher than the factor fresh traffic aerosol, are maximum during daytime but of less variability during the study period and of lesser magnitude than the secondary aerosol factor. The stationary combustion aerosol factor is dependent on temperature but is also weaker than the secondary aerosol factor.

The comparison of the different factors from PMF analyses of PSD data with those from PMF analyses of PM_1 composition shows that the factor secondary aerosol is maximum during those time periods when the PM_1 mass concentration fractions (see Figure 2) are maximum (phase 4 and group "High concentrations"). Finally, the same emission sources from both PMF analyses can be summarized (PSD / PM_1 composition) as shown in Figure S23:

- fresh traffic and aged traffic aerosol factor / BC and HOA (traffic factor or primary organic factor),
- stationary combustion aerosol factor / BC and WCOA (wood combustion factor),
- secondary aerosol factor / OOA (secondary organic factor).

Further, the secondary aerosol factor is correlated with $PM_{2.5}$ and PM_{10} , stationary combustion aerosol factor with NC100-500, aged traffic aerosol factor with NC50-100 and NC30-50, fresh traffic aerosol factor with NC10-30 and nucleation aerosol factor with NC3-10 which corresponds to the results in Tables 4 and 5 of Gu et al. (2012).

5 Summary, discussion and conclusions

5.1 Summary

5.1 Emissions

The temporal variations of gaseous air pollutants and PM composition as well as meteorological parameters during this high air pollution winter episode on the basis of hourly-mean data show characteristic temporal phases. These variations were mainly caused by weather changes as emission variation could never influence the concentrations of gaseous air pollutants and PM components to the degree (one order of magnitude) found during this study period. Source apportionment from PM_1 composition as well as from PSD in the size range from 3.8 nm to 800 nm of $PM_{2.5}$ -provided the main emission sources: road traffic as well as stationary and/or wood combustion (see Figure S23). This is in agreement with the real emissions in the surroundings of the measurement station (an urban background site, see section 2.2)-which are from residential areas. But The concentrations of the secondary aerosols factor are very often the higherst ones than those of road traffic as well as stationary and/or wood combustion. This agrees with the findings in Paris duringas also found in winter 2010 in Paris (Crippa et al., 2013).

Further, the cross-correlations of each air pollutant and PM component show two clusters: "secondary pollutants compounds of the PM_1 and fine particles" as well as "primary pollutants and accumulation mode particles".

5.2 Transport

The understanding of processes directing PMC, PNC and thus PSD as well as particle composition and thus secondary particle formation requires knowledge of the wind, MLH, humidity and temperature. The role of dilution and transport (wind speed), the mixing volume (MLH), particle growth (humidity), and secondary particle formation (temperature, humidity) could be shown quantitatively on the basis of correlation analyses. These two clusters, "secondary pollutants compounds of PM_1 and fine

particles" as well as "primary pollutants and accumulation mode particles" were also found by studying in the correlations between the concentration of each pollutant and meteorological parameters. Wind speed, MLH and relative humidity are important parameters influencing concentrations of primary pollutants as well as whereas temperature and humidity showed higher impact on concentrations of secondary pollutants. That means that transport or dispersion is relevant for locally or regionally emitted primary pollutants mainly. The investigation of the dependence of pollutant concentrations on wind direction provides information about the dominant role of wind speed and MLH highest concentrations of these pollutants were detected during wind directions from the crossing of two main roads in about 270 m distance to the Southeast (Figure 7).

5.3 Ozone

The sign of the correlation of ozone with the other air pollutants (mostly negative) and meteorological parameters is always opposite to the corresponding sign of all other pollutants. This is related to the photochemical formation of ozone – it is a secondary pollutant which is mainly formed from NO, NO₂ and volatile organic compounds – as well as titration.

5.4 Influence of meteorological parameters

OOA, secondary aerosol, NO₃⁻, SO₄²⁻, NH₄⁺, PM_{2.5}, PM₁₀ and stationary combustion aerosol (cluster "secondary pollutants-PM compounds and fine particles") and NC100-500 showed low concentrations during high absolute humidity and vice versa. All these compounds are more stable during low temperature and thus during low humidity (the lower the temperature the lower the absolute humidity; relative humidity is calculated for the maximum water vapour content at a certain temperature). Concentrations of other pollutants, these are primary pollutants like CO, benzene, HOA and BC as well as ultrafine particles, nucleation mode particles, fresh and aged traffic aerosols, showed nearly no dependence on absolute humidity. These pollutants are not chemically transformed or taking up water in the atmosphere so that the water vapour concentration has no influence on their concentration.

5.5 Special phase

Phase 4 is a short-term event with a strong PMC (particle mass concentration) increase during "wet" snow fall. Higher SO₄²⁻ and WCOA contents in comparison to the other phases exist were observed but NO₃⁻ was not enhanced. This could have been caused by more wood combustion.

The sign of the correlation of ozone with the other air pollutants (mostly negative) and meteorological parameters was always opposite to the corresponding sign of all other pollutants. This is related to the photochemical formation of ozone – it is a secondary pollutant which is mainly formed from NO, NO₂ and volatile organic compounds – as well as titration of ozone.

5.6 Conclusions

During high air pollution events, wind speed, mixing layer height, humidity, and temperature mainly influence the mass concentration of gaseous air pollutants and PM compounds as well as the particle size distribution. But the importance varies during different weather conditions. In general the role of different changes in emission sources strength was less important, meaning that the first hypothesis, that a dominant influence of meteorological parameters exists not only for gaseous pollutants but also for PM compounds composition and the particle size distribution, has been demonstrated. This is shown also from data of two different source apportionment analyses (PMF for PM₁ composition and PM_{2.5} size distribution). The PM₁₀ limit value exceedances were caused mainly by the meteorological influences and not only by the emissions. This is different during the

short-term phase 4 with snow fall and a strong influence of wood combustion emissions. On the other hand, the mass concentrations of toluene, NO, NC3-10 (nucleation mode particles), NC10-30, NC30-50 (Aitken mode particles) and fresh traffic aerosols, which are not part of the cluster "primary pollutants and accumulation mode particles" are only weakly dependent on meteorological parameters and seem to be driven by emissions. A further underlying mechanism is that This is supported by the fact that the specific particle size distribution during a relatively "clean" conditions, there are less air mass does not provide enough particle surfaces for coagulation of ultrafine particles which act as a sink for nucleation particles and to a lesser extent for Aitken mode particles (e.g., via coagulation). In this sense the first hypothesis is approved.

Three typical groups of pollution phases dependent from meteorological influences-parameters could be separated are identified. In the first group is low to average mass concentrations (PM₁, PM_{2,5}, PM₁₀) with higher organic and SO₄²⁻ content as well as high NO₃⁻ content in PM₁ concentration were observed peaks together with peak concentrations of CO, NO and NO_x. These phases were concentrations occurring during periods with varying temperature, wind speeds between 1 and 11 m/s and northerly wind directions (influence of city centre, but not for NO and NO_x). The second group was is characterized by high mass concentrations (PM₁, PM_{2,5}, PM₁₀ and 6 of the 8 PM₁₀ limit value exceedances) with higher organic and SO₄²⁻ content as well as high NO₃⁻ content in PM₁ concentration peaks accompanied by the highest detected CO, NO and NO_x concentrations. During these periods were characterized by temperatures mostly below 0°C, the lowest wind speeds (below 7 m/s) and often south-easterly wind directions (influence of road traffic). In the third group is very low mass concentrations (PM₁, PM_{2,5}, PM₁₀) with high organic content in PM₁ with some peak CO, NO and NO_x concentrations were observed during the highest temperatures (up to +13°C), the highest wind speeds (up to 14 m/s) and wind directions from west-southwest to south-southeast (influence of university and residential areas). This shows the well-known influences of emissions, advection and mixing upon PM compound and air pollutant concentrations as well as of emissions and temperature upon chemical composition of ambient air and PM with some specifics in the case of the sampling site in Augsburg.

Two clusters – primary pollutants and secondary pollutants-PM components – are important since the influence of the meteorological parameters determined by correlations is different (but always significant): wind speed (negative), wind direction, mixing layer height (negative) and relative humidity (positive) influence primary pollutants and accumulation mode particle concentrations whereas as well as temperature (negative), and absolute humidity (negative) and also relative humidity (positive) influence secondary pollutants-PM component and fine particle concentrations. Correlations indicate the new result that secondary pollutants-PM compound concentrations depend on absolute humidity also and primary pollutant concentrations on relative humidity only. This means that secondary aerosol forming processes are dependent from meteorological parameters including absolute humidity. Consequently, also the second hypothesis is correct.

Ultra-fine particle (particle diameter < 100 nm) exposures, which are of high health risk, are only weakly dependent on meteorological parameters and are thus influenced by emissions and secondary particle formation processes. The determination of the meteorological influences upon the air pollution exposure by correlation analyses, which is shown here, can explain major parts of certain PM compound and air pollutant exposure. These influences were investigated already by Tai et al. (2010) for PM_{2,5} concentrations, but not for PM compounds and gaseous air pollutants, Wen et al. (2010) for air pollutants, but not for PM compounds, Wu et al. (2013) for daily mean values only

and Tandon et al. (2010) for eight-hourly mean data only. The topic of meteorological influences upon nearly all air pollutants is studied in a comprehensive view with high temporal resolved data for the first one. The new results, presented here on the basis of hourly-mean data (4 PM compounds, 7 gaseous pollutants and VOC, 2 size fraction mass modes and 5 number concentration modes as well as 8 PM source factors) and thus daily variations, provide more implications for the sensitivity of PM compounds and gaseous air pollutants to meteorological parameters and as a consequence to a change of climate. General circulation and chemistry transport models which are applied to calculate such influences of climate change upon air quality need detailed information about the processes to be simulated. The statistical investigations of meteorological influences upon PM compounds and gaseous air pollutants as shown here for nearly all air pollutants provide such information in the present atmosphere (see also Tai et al., 2010).

The application of various complex statistical methods to analyse measured ambient air data was advantageous because an alternatively applied tropospheric chemical model requires a good emission inventory which is not available real time normally. Further, a scaling problem exists. Appropriate to the point measurements, a small-scale or box model is required with a corresponding emission inventory which must be calculated also.

The results presented here concerning high air pollutant concentrations contribute to general information for aiding epidemiological investigations performed in this urban area (Cyrus et al., 2008; Gu et al., 2012).

The determined meteorological influences upon PM compounds and gaseous air pollutants provide detailed basic information which is necessary and for the development of emission reduction measures of certain compounds.

Acknowledgements

We like to thank our colleagues C. Jahn, R. Friedl and M. Hoffmann (KIT/IMK-IFU) for effective cooperation during the measurement campaign, Christoph Münkel (Vaisala GmbH, Hamburg, Germany) for cooperation within the frame of MLH determination from ceilometer data and Michael Tuma (KIT/IMK-IFU) during his internship for careful MLH analyses from ceilometer and RASS measurements. We are very thankful for the the language corrections (both grammar and comprehensibility) of the manuscript by Richard Foreman (KIT/IMK-IFU). We acknowledge support by Deutsche Forschungsgemeinschaft and Open Access Publishing Fund of Karlsruhe Institute of Technology.

References

Aiken, A. C., DeCarlo, P. F., Kroll, J. H., Worsnop, D. R., Huffman, J. A., Docherty, K., Ulbrich, I. M., Mohr, C., Kimmel, J. R., Sueper, D., Zhang, Q., Sun, Y., Trimborn, A., Northway, M., Ziemann, P. J., Canagaratna, M. R., Onasch, T. B., Alfarra, R., Prévôt, A. S. H., Dommen, J., Duplissy, J., Metzger, A., Baltensperger, U., and Jimenez, J. L.: O/C and OM/OC Ratios of Primary, Secondary, and Ambient Organic Aerosols with High Resolution Time-of-Flight Aerosol Mass Spectrometry, *Environ. Sci. Technol.*, 42, 4478-4485, 2008.

Alföldy, B., Osán, J., Tóth, Z., Török, S., Harbusch, A., Jahn, C., Emeis, S., and Schäfer, K.: Aerosol optical depth, aerosol composition and air pollution during summer and winter conditions in Budapest, *Sci. Total Environ.*, 383, 141-163, 2007.

Allan, J. D., Delia, A. E., Coe, H., Bower, K. N., Alfarra, M. R., Jimenez, J. L., Middlebrook, A. M., Drewnick, F., Onasch, T. B., Canagaratna, M. R., Jayne, J. T., and Worsnop, D. R.: A generalised method for the extraction of chemically resolved mass spectra from Aerodyne aerosol mass spectrometer data, *J. Aerosol Sci.*, 35, 909-922, 2004.

Barmpadimos, I., Hueglin, C., Keller, J., Henne, S., and Prévôt, A. S. H.: Influence of meteorology on PM10 trends and variability in Switzerland from 1991 to 2008, *Atmos. Chem. Phys.*, 11, 1813-1835, 2011.

Barmpadimos, I., Keller, J., Oderbolz, D., Hueglin, D., and Prévôt, A. S. H.: One decade of parallel fine (PM2.5) and coarse (PM10–PM2.5) particulate matter measurements in Europe: trends and variability, *Atmos. Chem. Phys.*, 12, 3189-3203, 2012.

Birmili, W., Stratmann, F., and Wiedensohler, A.: Design of a DMA-based size spectrometer for a large particle size range and stable operation, *J. Aerosol Sci.* 30, 549-553, 1999.

Birmili, W., Weinhold, K., Nordmann, S., Wiedensohler, A., Spindler, G., Müller, K., Herrmann, H., Gnauk, T., Pitz, M., Cyrys, J., Flentje, H., Nickel, C., Kuhlbusch, T.A.J. Löschau, G., Haase, D., Meinhardt, F., Schwerin, A., Ries, L., and Wirtz, K.: Atmospheric aerosol measurements in the German Ultrafine Aerosol Network (GUAN): Part 1 - soot and particle number size distributions, *Gefahrst. Reinhalt. L.*, 69, 137-145, 2009.

Crippa, M., DeCarlo, P.F., Slowik, J.G., Mohr, C., Heringa, M.F., Chirico, R., Poulain, L., Freutel, F., Sciare, J., Cozic, J., Di Marco, C.F., Elsasser, M., Nicolas, J.B., Marchand, N., Abidi, E., Wiedensohler, A., Drewnick, F., Schneider, J., Borrmann, S., Nemitz, E., Zimmermann, R., Jaffrezo, J.-L., Prevot, A.S.H., and Baltensperger, U.: Wintertime aerosol chemical composition and source apportionment of the organic fraction in the metropolitan area of Paris, *Atmos. Chem. Phys.*, 13, 961–981, 2013.

Cyrys, J., Pitz, M., Heinrich, H., Wichmann, H. E., and Peters, A.: Spatial and temporal variation of particle number concentration in Augsburg, Germany, *Sci. Total Environ.*, 401, 168-175, 2008.

DeCarlo, P. F., Dunlea, E. J., Kimmel, J. R., Aiken, A. C., Sueper, D., Crounse, J., Wennberg, P. O., Emmons, L., Shinozuka, Y., Clarke, A., Zhou, J., Tomlinson, J., Collins, D. R., Knapp, D., Weinheimer, A. J., Montzka, D. D., Campos, T., and Jimenez, J. L.: Fast airborne aerosol size and chemistry measurements above Mexico City and Central Mexico during the MILAGRO campaign, *Atmos. Chem. Phys.*, 8, 4027-4048, 2008.

Donateo, A., Contini, D., Belosi, F., Gambarano, A., Santachiara, G., Cesari, D., and Prodi, F.: Characterisation of PM2.5 concentrations and turbulent fluxes on a island of the Venice lagoon using high temporal resolution measurements, *Meteorol. Z.*, 21, 4, 385-398, 2012.

Directive 2008/50/EC: Directive 2008/50/EC of the European parliament and of the council of 21 May 2008 on ambient air quality and cleaner air for Europe, Official Journal of the European Union, L 152/2, 11.6.2008.

El-Metwally, M. and Alfaro, S.C.: Correlation between meteorological conditions and aerosol characteristics at an East-Mediterranean coastal site, *Atmos. Res.*, 132-133, 76–90, 2013.

Elsasser, M., Crippa, M., Orasche, J., DeCarlo, P.F., Oster, M., Pitz, M., Cyrys, J., Gustafson, T.L., Pettersson, J.B.C., Schnelle-Kreis, J., Prévôt, A.S.H., and Zimmermann, R.: Organic molecular markers and signature from wood combustion particles in winter ambient aerosols: aerosol mass spectrometer (AMS) and high time-resolved GC-MS measurements in Augsburg, Germany, *Atmos. Chem. Phys.*, 12, 6113–6128, 2012.

Emeis, S., Münkel, C., Vogt, S., Müller, W., and Schäfer, K.: Determination of mixing-layer height, *Atmos. Environ.*, 38, 273-286, 2004.

Emeis, S. and Schäfer, K.: Remote sensing methods to investigate boundary-layer structures relevant to air pollution in cities, *Bound-Lay. Meteorol.*, 121, 377-385, 2006.

Emeis, S., Jahn, C., Münkel, C., Münsterer, C., and Schäfer, K.: Multiple atmospheric layering and mixing-layer height in the Inn valley observed by remote sensing, *Meteorol. Z.*, 16, 415-424, 2007.

Emeis, S., Schäfer, K., and Münkel, C.: Surface-based remote sensing of the mixing-layer height – a review, *Meteorol. Z.*, 17, 621-630, 2008.

Emeis, S., Schäfer, K., and Münkel, C.: Observation of the structure of the urban boundary layer with different ceilometers and validation by RASS data, *Meteorol. Z.* 18, 149-154, 2009.

Emeis, S., Schäfer, K., Münkel, C., Friedl, R., and Suppan, P.: Evaluation of the interpretation of ceilometer data with RASS and radiosonde data, *Bound-Lay. Meteorol.*, 143, 25–35, 2012.

Gu, J. W., Pitz, M., Schnelle-Kreis, J., Diemer, J., Reller, A., Zimmermann, R., Soentgen, J., Stoelzel, M., Wichmann, H. E., Peters, A., and Cyrys, J.: Source apportionment of ambient particles: Comparison of positive matrix factorization analysis applied to particle size distribution and chemical composition data, *Atmos. Environ.*, 45, 1849–1857, 2011.

Gu, J., Pitz, M., Breitner, S., Birmili, W., von Klot, S., Schneider, A., Soentgen, J., Reller, A., Peters, A., and Cyrys, J.: Selection of key ambient particulate variables for epidemiological studies — Applying cluster and heatmap analyses as tools for data reduction, *Sci. Total Environ.*, 435-436, 541–550, 2012.

Helmis, C.G., Sgouros, G., Tombrou, M., Schäfer, K., Münkel, C., Bossiolo, E., and Dandou, A.: A comparative study and evaluation of Mixing Height estimation based on SODAR-RASS, ceilometer data and model simulations, *Bound-Lay. Meteorol.*, 145, 507–526, 2012.

Jacobeit, J.: Stadtklimatologie von Augsburg unter besonderer Berücksichtigung der lufthygienischen Situation sowie des Lärms, Forschungsprojekt im Auftrag und mit Förderung der Stadt Augsburg, In: Fischer K. [Hrsg.]: Augsburger Geographische Hefte, 6, 171 pp, 1986.

Ji, D.S., Li, L., Wang, Y.S., Zhang, J., Cheng, M.T., Sun, Y., Liu, Z., Wang, L., Tang, G.Q., Hu, B., Chao, N., Wen, T.X., Miao, H.Y.: The heaviest particulate air-pollution episodes occurred in northern China in January, 2013: Insights gained from observation. *Atmos. Environ.*, DOI: 10.1016/j.atmosenv.2014.04.048.

Lanz, V. A., Alfarra, M. R., Baltensperger, U., Buchmann, B., Hueglin, C., and Prevot, A. S. H.: Source apportionment of submicron organic aerosols at an urban site by linear unmixing of aerosol mass spectra, *Atmos. Chem. Phys.*, 7, 1503-1522, 2007.

Liu, X., Gu, J., Li, Y., Cheng, Y., Qu, Y., Han, T., Wang, J., Tian, H., Chen, J., and Zhang, Y.: Increase of Aerosol Scattering by Hygroscopic Growth: Observation, Modeling, and Implications on Atmospheric Visibility, *Atmos. Res.*, 132, 91-101, 2013.

Malm, W.C. and Day, D.E.: Estimates of aerosol species scattering characteristics as a function of relative humidity, *Atmos. Environ.*, 35, 2845-2860, 2001.

Münkel, C.: Mixing height determination with lidar ceilometers - results from Helsinki Testbed, *Meteorol. Z.*, 16, 451-459, 2007.

Münkel, C., Schäfer, K., and Emeis, S.: Confidence levels and error bars for continuous detection of mixing layer heights by ceilometer. In: Extended Abstracts of Presentations from the 16th International Symposium for the Advancement of Boundary-Layer Remote Sensing, 5-8 June 2012, Boulder, CO USA, 98-101, 2012.

Paatero, P. and Tappert U.: Positive Matrix Factorization: a non-negative factor model with optimal utilization of error estimated of data values, *Environmetrics*, 5, 111-126, 1994.

Paatero, P.: Least squares formulation of robust non-negative factor analysis, *Chemometr. Intell. Lab.*, 37, 23–35, 1997.

Pitz, M., Birmili, W., Schmid, O., Peters, A., Wichmann, H.E., and Cyrys, J.: Quality control and quality assurance for particle size distribution measurements at an urban monitoring station in Augsburg, Germany, *J. Environ. Mon.*, 10, 1017-1024, 2008.

Rückerl, R., Schneider, A., Breitner, S., Cyrys, J., and Peters, A.: Health Effects of Particulate Air Pollution – A Review of Epidemiological Evidence, *Inhal. Toxicol.*, 23(10), 555–592, 2011.

Schäfer, K., Emeis, S., Hoffmann, H., and Jahn, C.: Influence of mixing layer height upon air pollution in urban and sub-urban areas, *Meteorol. Z.*, 15, 647-658, 2006.

Schäfer, K., Emeis, S., Schrader, S., Török, S., Alfoldy, A., Osan, J., Pitz, M., Münkel, C., Cyrys, J., Peters, A., Sarigiannis, D., and Suppan, P.: A measurement based analysis of the spatial distribution, temporal variation and chemical composition of particulate matter in Munich and Augsburg, *Meteorol. Z.*, 21, 47-57, 2011.

Schäfer, K., Pitz, M., Höss, M., Friedl, R., Emeis, S., Münkel, C., Cyrys, J., Schrader, S., Hoffmann, M., Jahn, C., Jacobbeit, J., Peters, A., Soentgen, J., and Suppan, P.: Investigation of meteorological influences and mixing-layer height upon ultrafine particle size distribution in the urban area of Augsburg, In: Book of Abstracts, 8th International Conference on Air Quality. Science and Application, Athens, Greece, 19-23 March 2012, University of Hertfordshire, 121, ISBN: 978-1-907396-80-9, 2012.

Stat. Jahrbuch: Statistisches Jahrbuch der Stadt Augsburg, online available at:
http://www.augsburg.de/fileadmin/user_upload/buergerservice_rathaus/rathaus/statistiken_und_geodaten/statistiken/jahrbuch/jahrbuch_2012.pdf (last access day 23 January 2014), 2013.

Sueper, D.: ToF-AMS High Resolution Analysis Software - Pika, online available at:
<http://cires.colorado.edu/jimenez-group/ToFAMSResources/ToFSoftware/PikaInfo/> (last access day 23 January 2014), 2010.

Tai, A.P.K., Mickley, L.J., and Jacob, D.J.: Correlations between fine particulate matter (PM2.5) and meteorological variables in the United States: Implications for the sensitivity of PM2.5 to climate change, *Atmos. Environ.*, 44, 3976-3984, 2010.

Tandon, A., Yadav, S., and Attri, A.K.: Coupling between meteorological factors and ambient aerosol load, *Atmos. Environ.*, 44, 1237-1243, 2010.

Ulbrich, I. M., Canagaratna, M. R., Zhang, Q., Worsnop, D. R., and Jimenez, J. L.: Interpretation of organic components from Positive Matrix Factorization of aerosol mass spectrometric data, *Atmos. Chem. Phys.*, 9(9), 2891-2918, 2009.

Ward, J.H.: Hierarchical grouping to optimize an objective function, *J. Am. Stat. Assoc.*, 58, 236-244, 1963.

Wagner, P.: Analyse von biogenem und anthropogenem Isopren und seiner Bedeutung als Ozonvorläufersubstanz in der Stadtatmosphäre, Inaugural-Dissertation zur Erlangung des Doktorgrades Dr. rer. nat. der Fakultät für Biologie an der Universität Duisburg-Essen, 2014.

Wen, C.-C. and Yeh, H.-H.: Comparative influences of airborne pollutants and meteorological parameters on atmospheric visibility and turbidity, *Atmos. Res.*, 96, 496–509, 2010.

Wu, S., Deng, F., Wang, X., Wei, H., Shima, M., Huang, J., Lv, H., Hao, Y., Zheng, C., Qin, Y., Lu, X., and Guo, X.: Association of Lung Function in A Panel of Young Healthy Adults with Various Chemical Components of Ambient Fine Particulate Air Pollution in Beijing, China, *Atmos. Environ.*, 77, 873-884, 2013.

Zhang, Q.H., Zhang, J.P., and Xue, H.W.: The challenge of improving visibility in Beijing, *Atmos. Chem. Phys.*, 10, 7821–7827, 2010.

Zhao, P., Zhang, X., Xu, X., and Zhao X.: Long-term visibility trends and characteristics in the region of Beijing, Tianjin, and Hebei, China, *Atmos. Res.*, 101, 711–718, 2011.

Yue, D., Hu, M., Wu, Z., Wang, Z., Guo, S., Wehner, B., Nowak, A., Achtert, P., Wiedensohler, A., Jung, J., Kim, Y.J., and Liu, S.: Characteristics of aerosol size distributions and new particle formation in the summer in Beijing, *J. Geophys. Res.*, 114, D00G12, doi:10.1029/2008JD010894, 2009.

Table 1. Correlation coefficients R^2 of hourly-mean values of NO and NO_x concentrations measured at the station Bourgesplatz with the measured concentrations at the stations LfU and urban edge background site (AVA), O_3 and CO concentrations measured at the station LfU with the measured concentrations at the urban edge background site (AVA) as well as $PM_{2.5}$ and PM_{10} concentrations measured at the station LfU with the urban background site (HSA). More details are in Figure S1. No correlations are given if no data are available.

Site	NO	NO_x	O_3	CO	$PM_{2.5}$	PM_{10}
AVA	0.45	0.60	0.88	0.78		
HSA					0.93	0.86
Bourgesplatz	1	1				
LfU	0.54	0.65	1	1	1	1

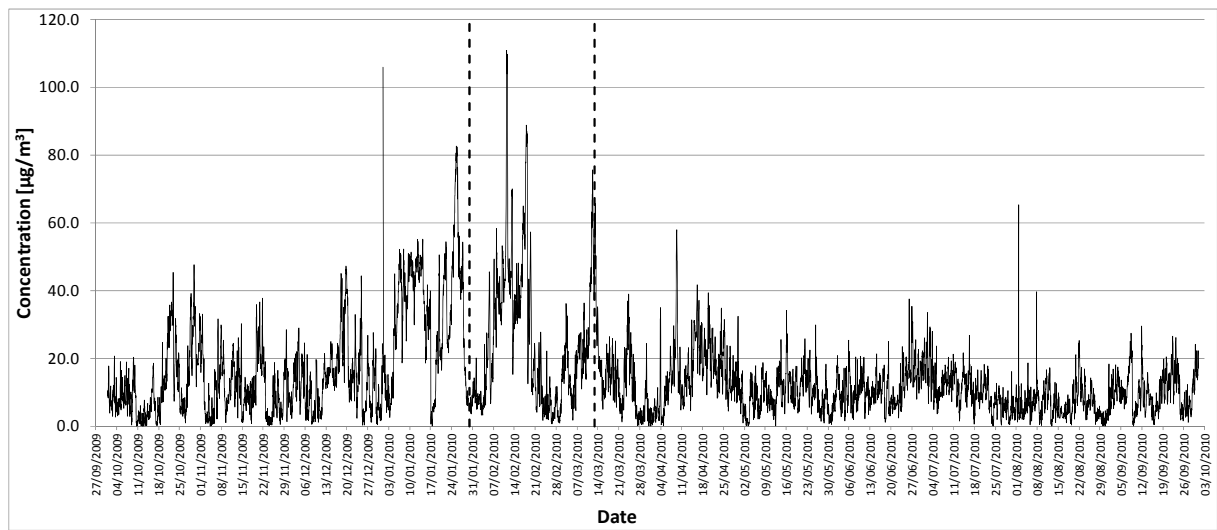


Figure 1. Time series of hourly-mean values of PM_{2.5} concentration measurements at the urban background site HSA from 01 October 2009 to 30 September 2010. The measurement period from 31 January, 00:00 CET to 12 March 2010, 24:00 CET is indicated by dashed lines.

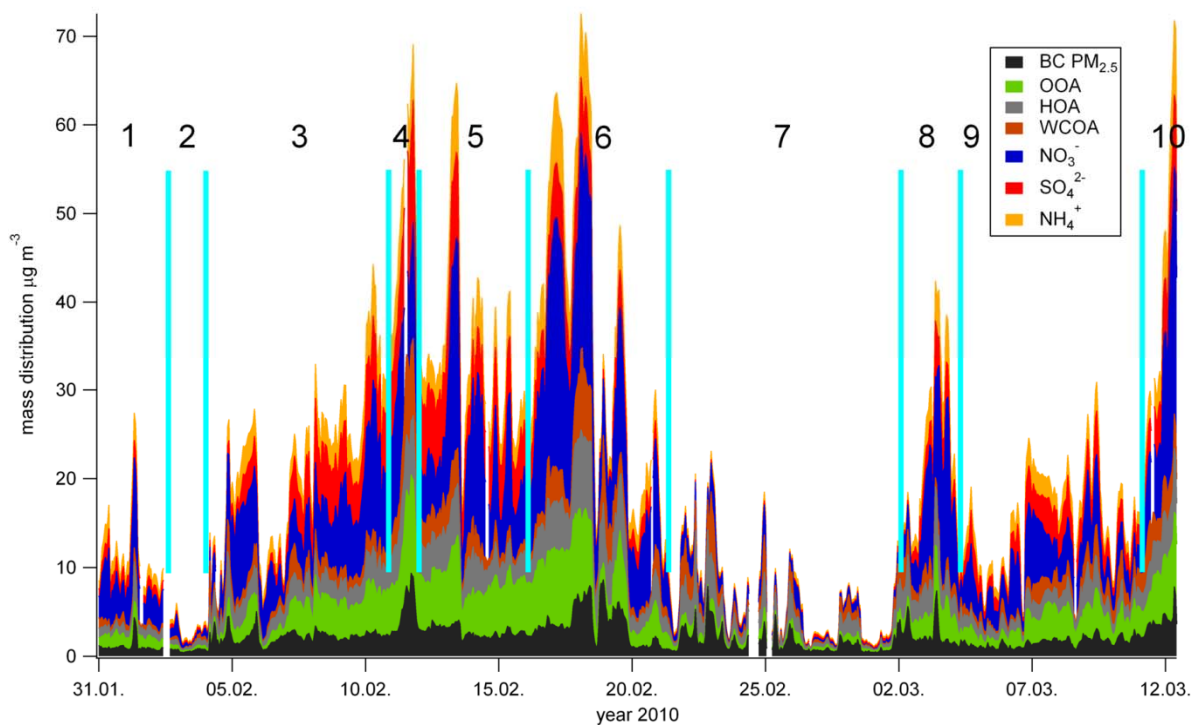


Figure 2. 10 temporal phases of PM_1 fractions (non-refractory particle components and PMF factors) and BC from $\text{PM}_{2.5}$ on the basis of hourly-mean values measured at the urban background site HSA (data source from Elsasser et al. (2012)): BC - black carbon, OOA - oxygenated organic aerosol, HOA - hydrocarbon-like organic aerosol, WCOA - wood combustion organic aerosol, NO_3^- - nitrate, SO_4^{2-} - sulphate, and NH_4^+ - ammonium (see text and Table S1S in the supplements). The border of the phases are coloured in light blue.

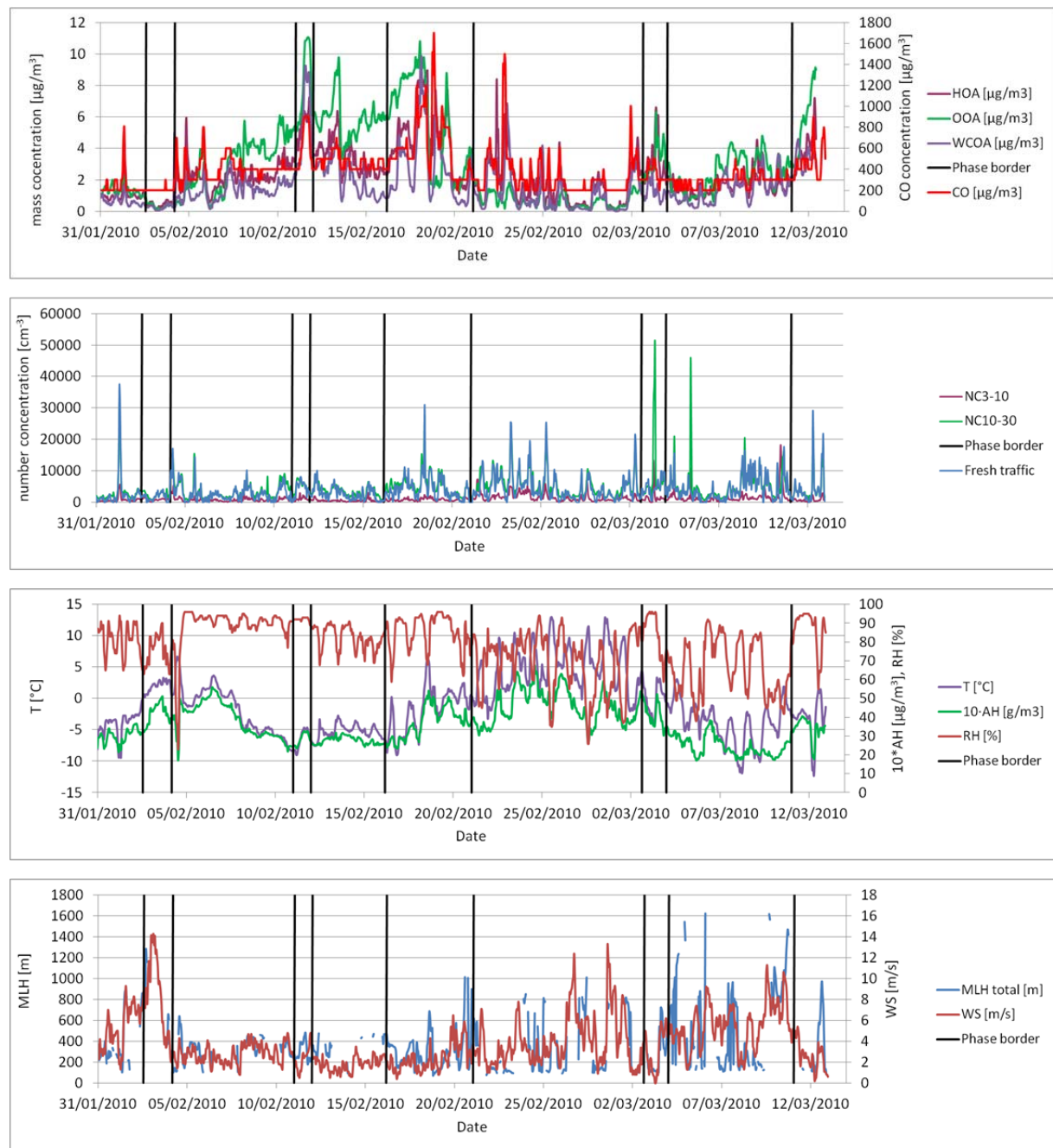


Figure 3. Temporal variation of OOA (oxygenated organic aerosol), HOA (hydrocarbon-like organic aerosol), WCOA (wood combustion organic aerosol) and CO concentrations (above), NC3-10, NC10-30 and the fresh traffic aerosol factor (second from above) together with the meteorological parameters T (temperature), RH (relative humidity) and AH (absolute humidity) (third from above) and WS (wind speed) and mixing layer height (MLH) (below). The borders of the 10 phases are drawn too.

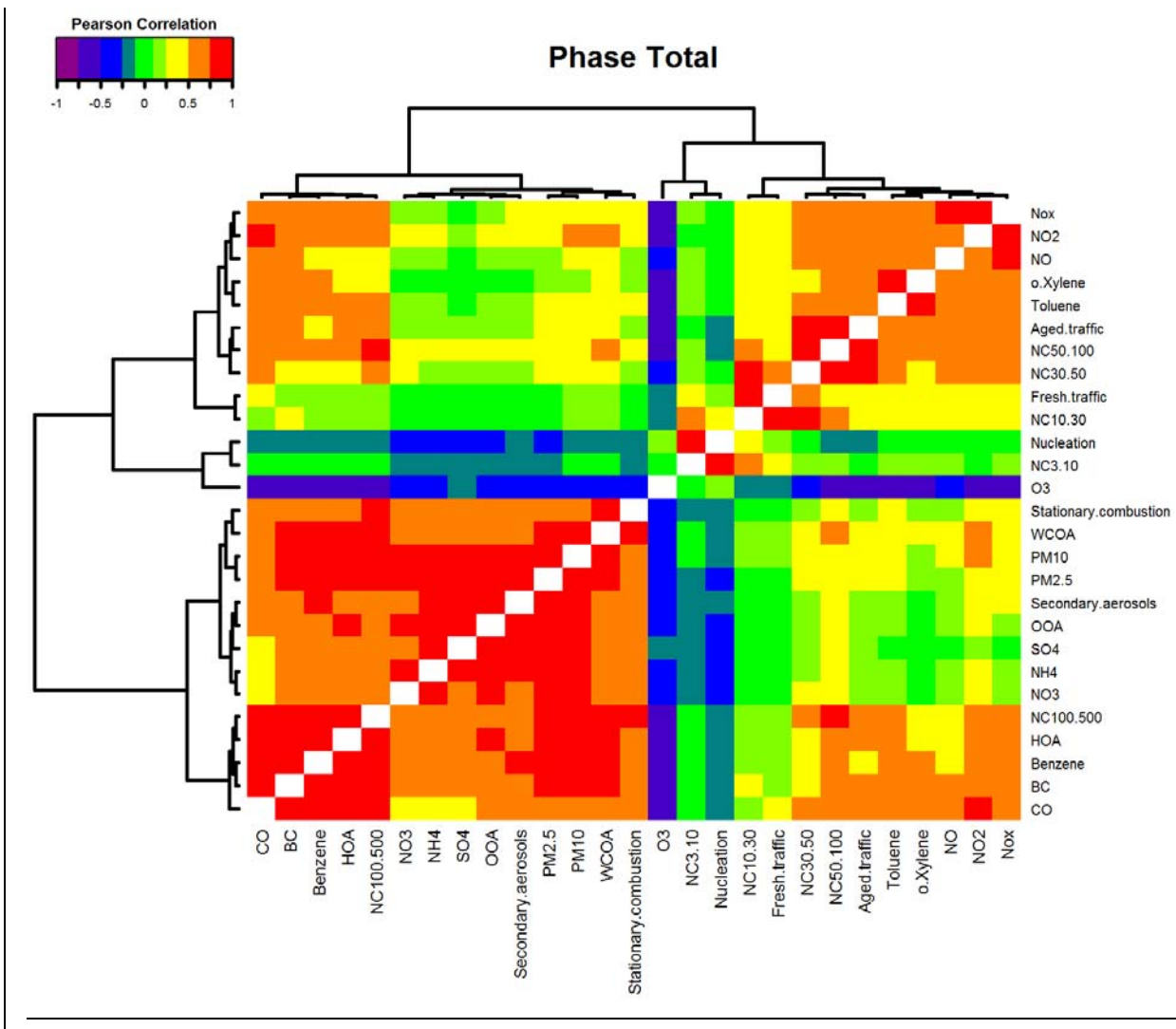
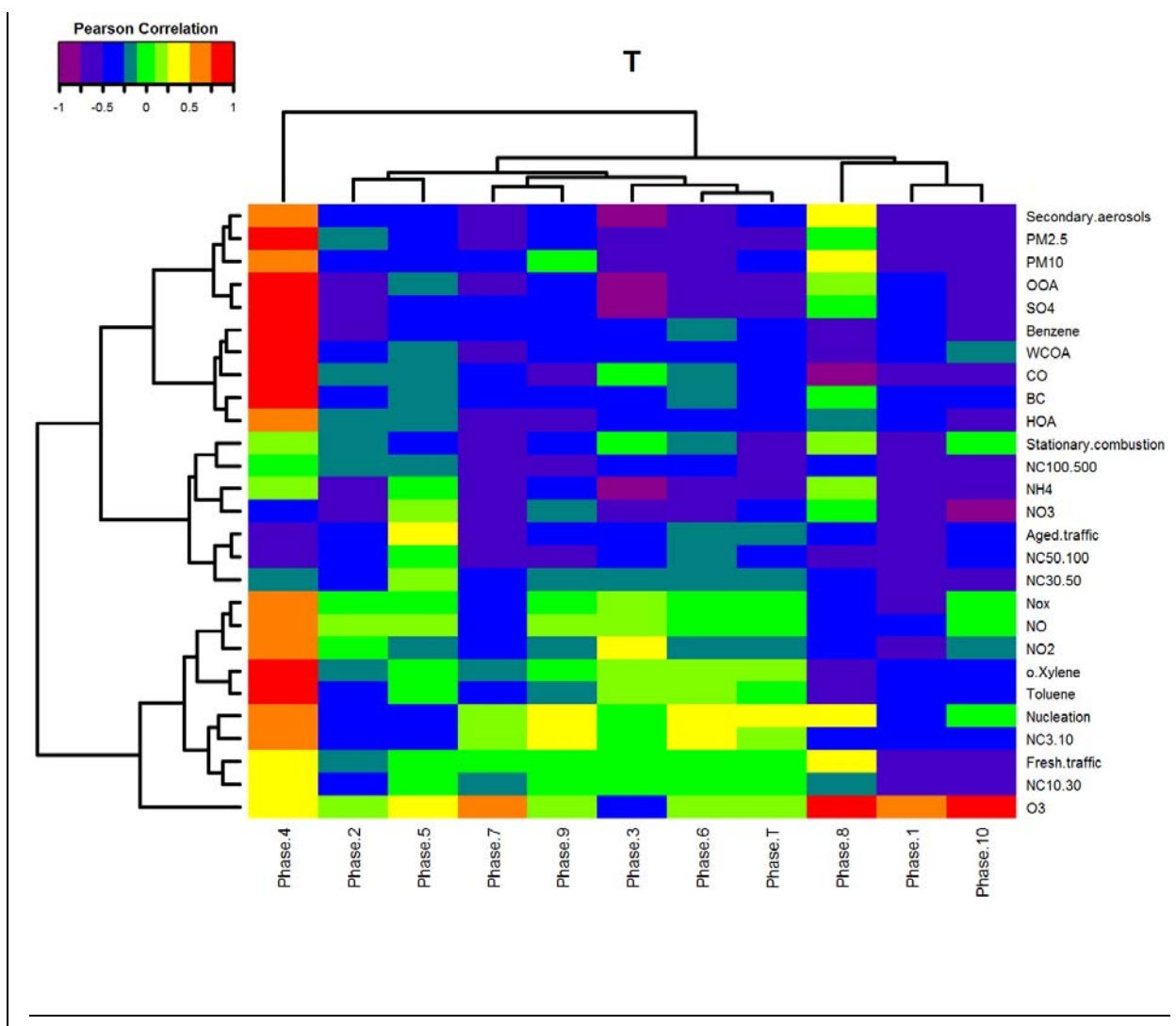
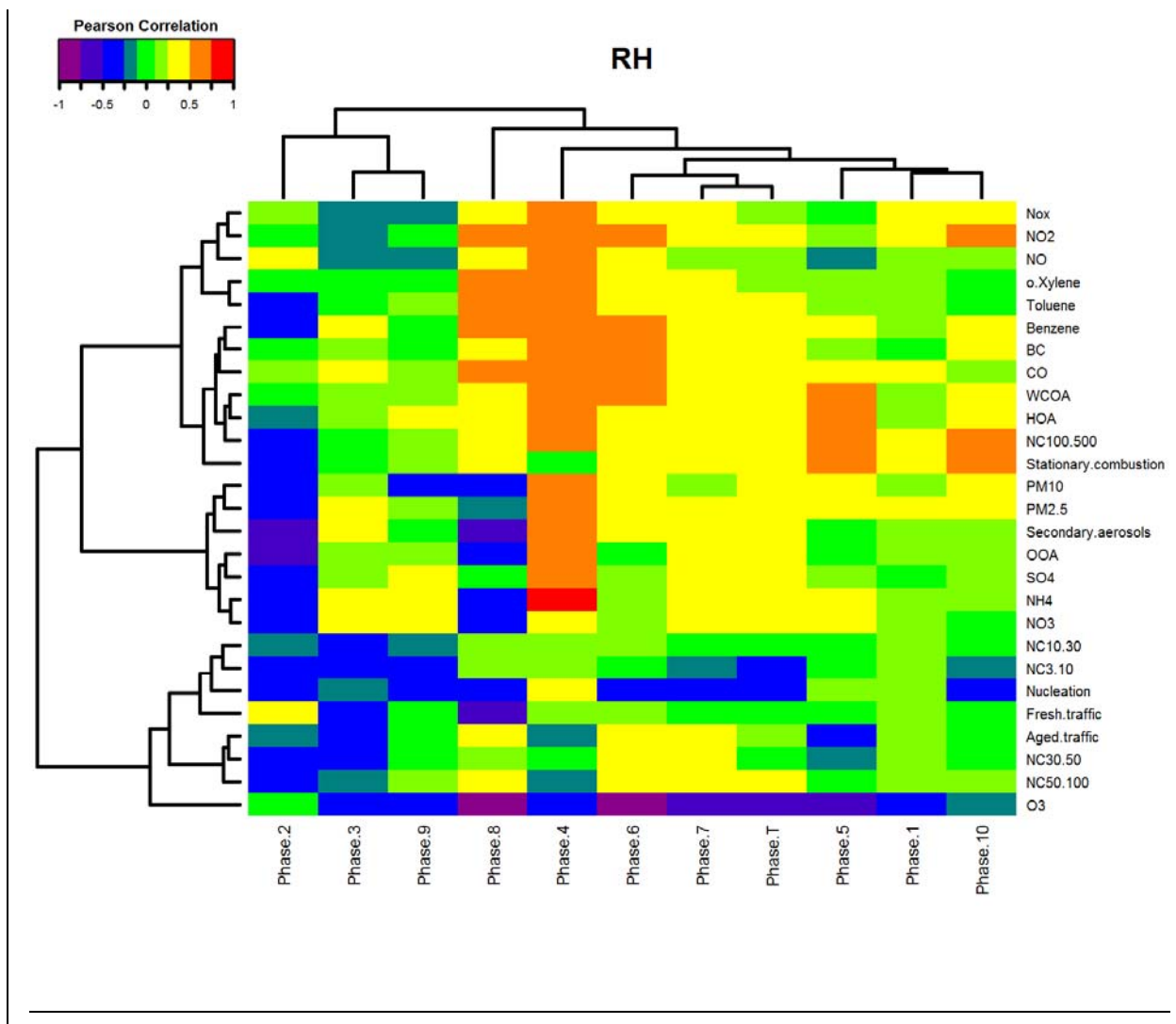
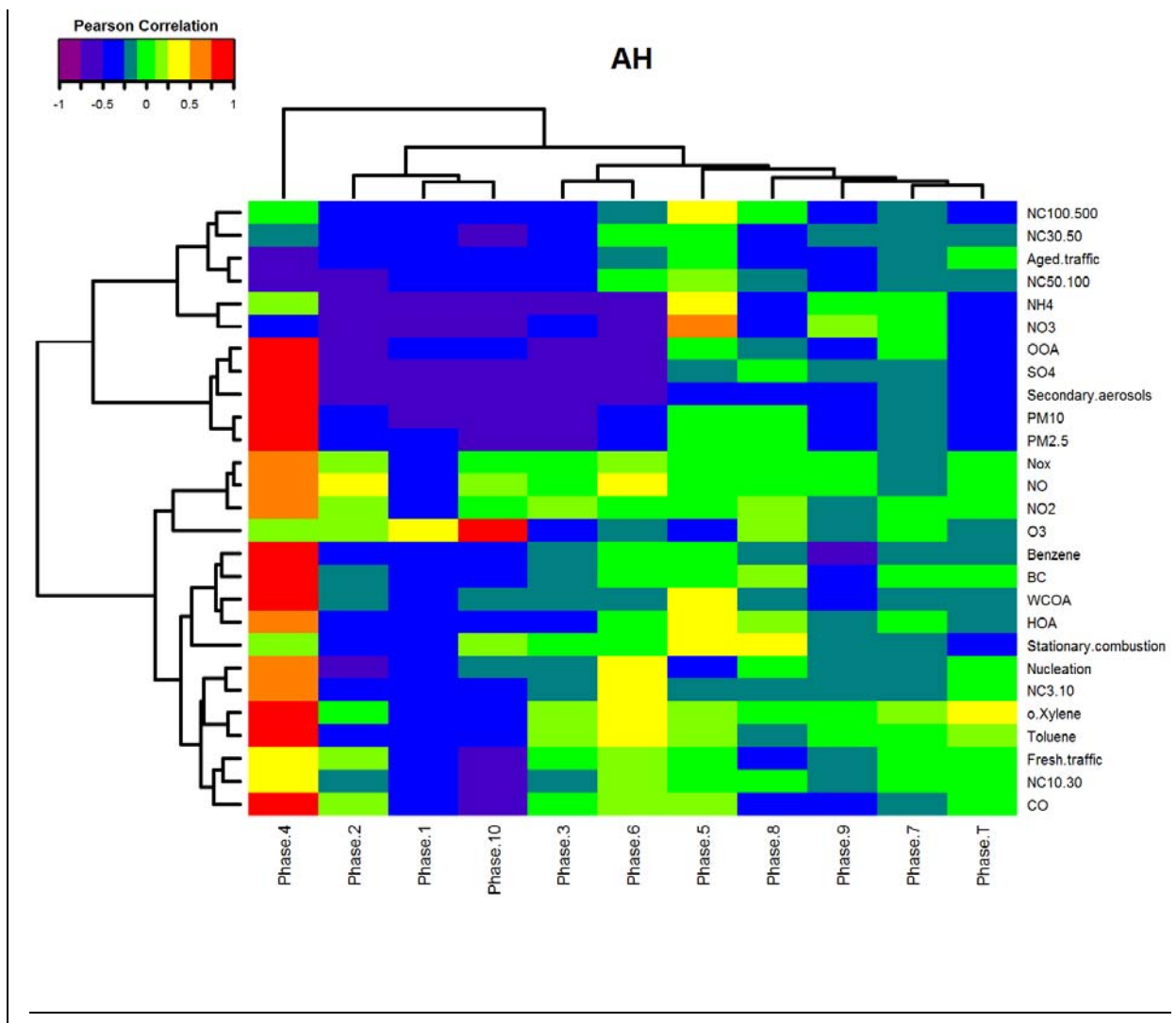
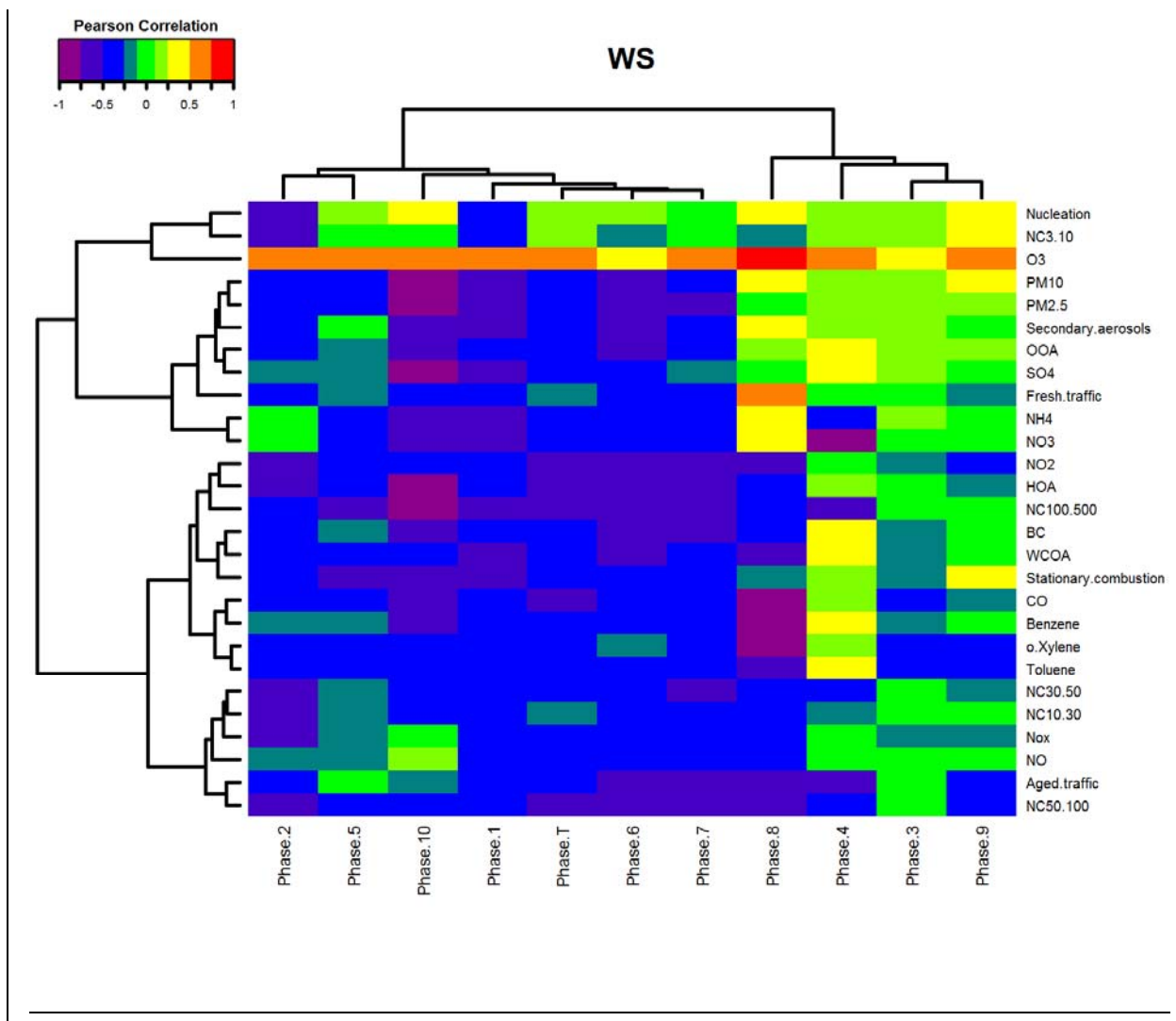


Figure 4. Heatmap with Pearson intercorrelations between all pollutants during the total measurement period (all temporal phases) showing different clusters including the two-dimensional dendrogram on the rows and columns. The correlations are coloured according to the scale on the top-left corner. Correlations between the same variables (equal to 1) are shown in white.









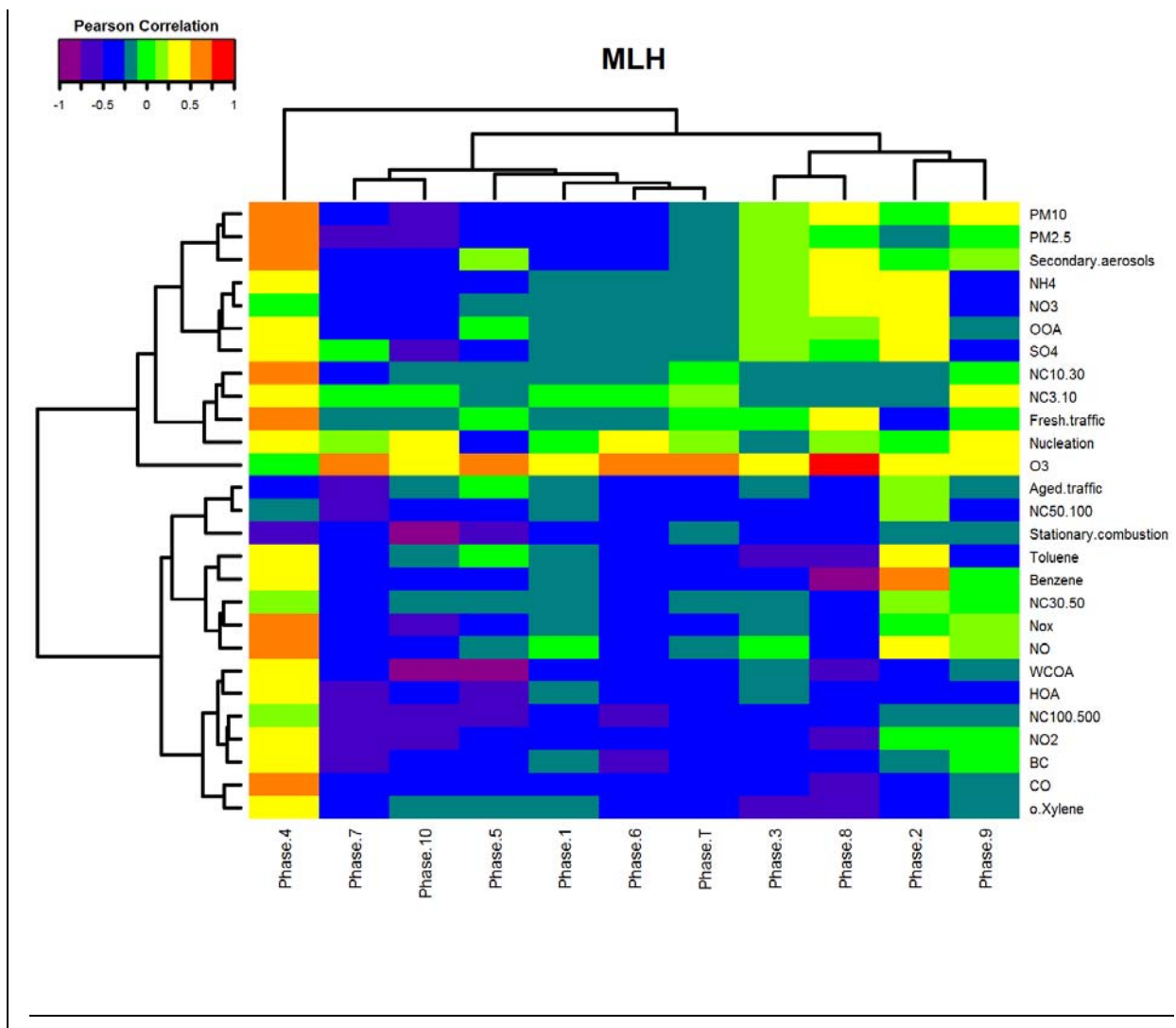
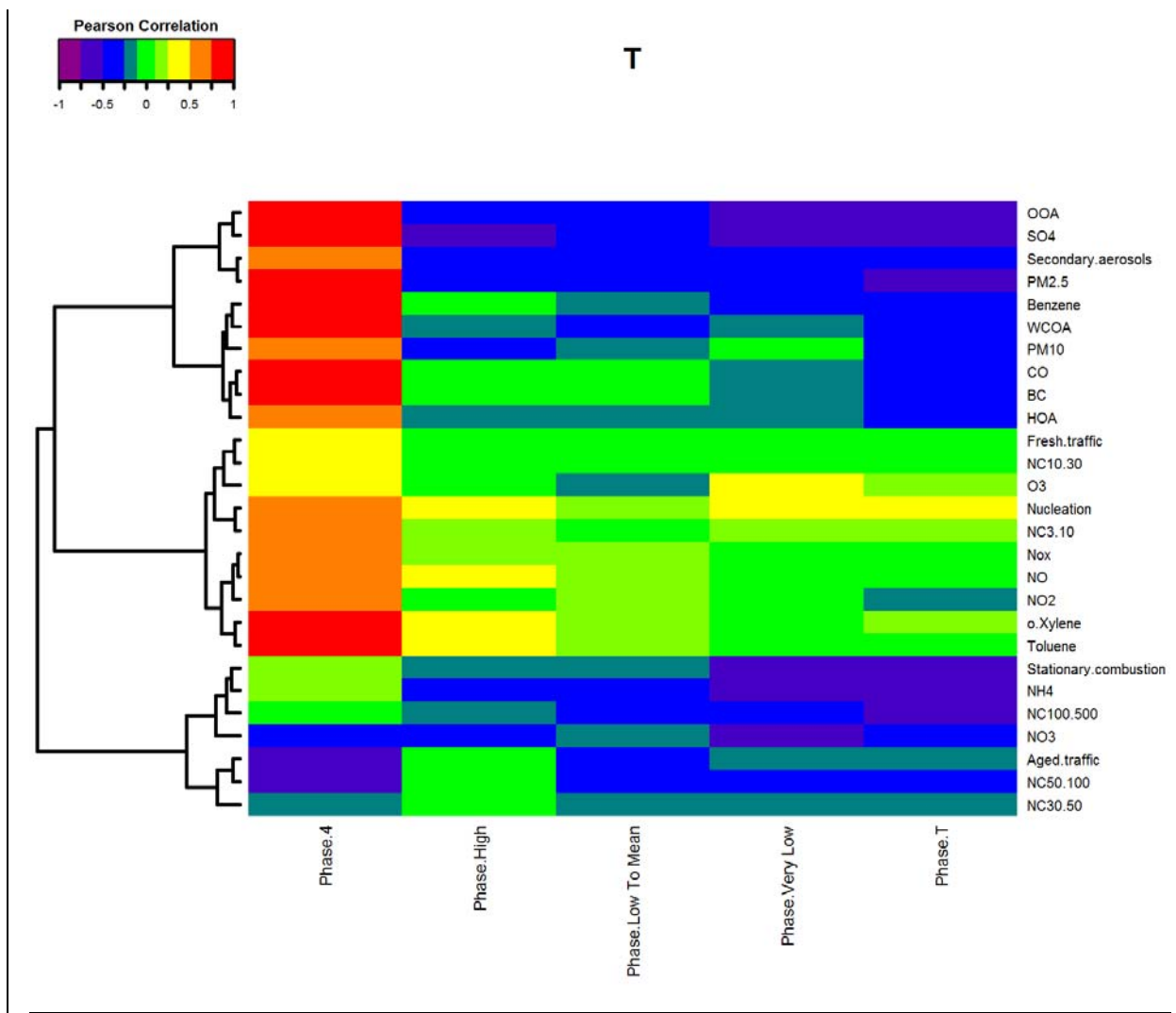
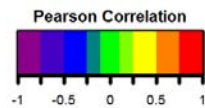
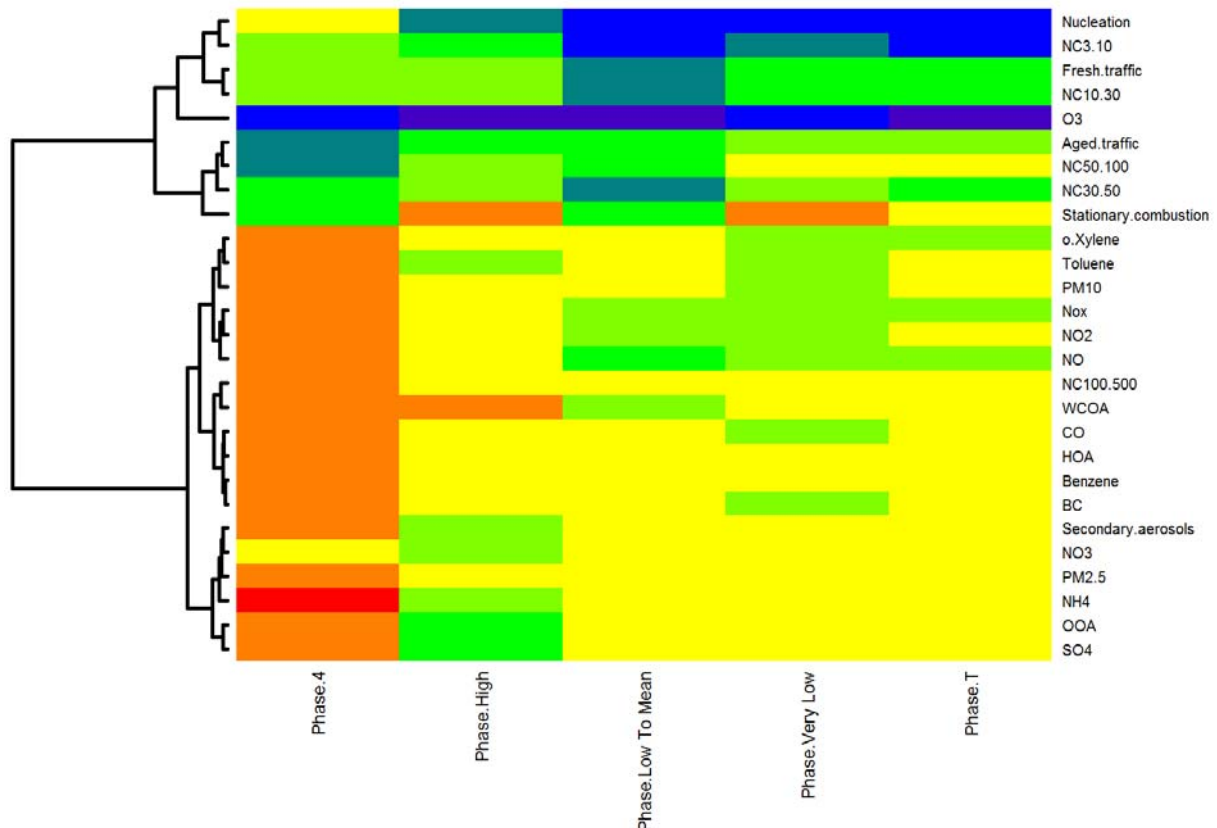


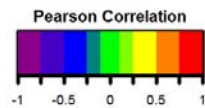
Figure 5. Heatmap with Pearson intercorrelations between pollutants and meteorological parameters (T (temperature), RH (relative humidity), AH (absolute humidity), WS (wind speed), MLH (mixing layer height)) during the total measurement period (each temporal phase and total period) showing different clusters including the dendrogram on the columns and rows. The correlations are coloured according to the scale on the top-left corner.



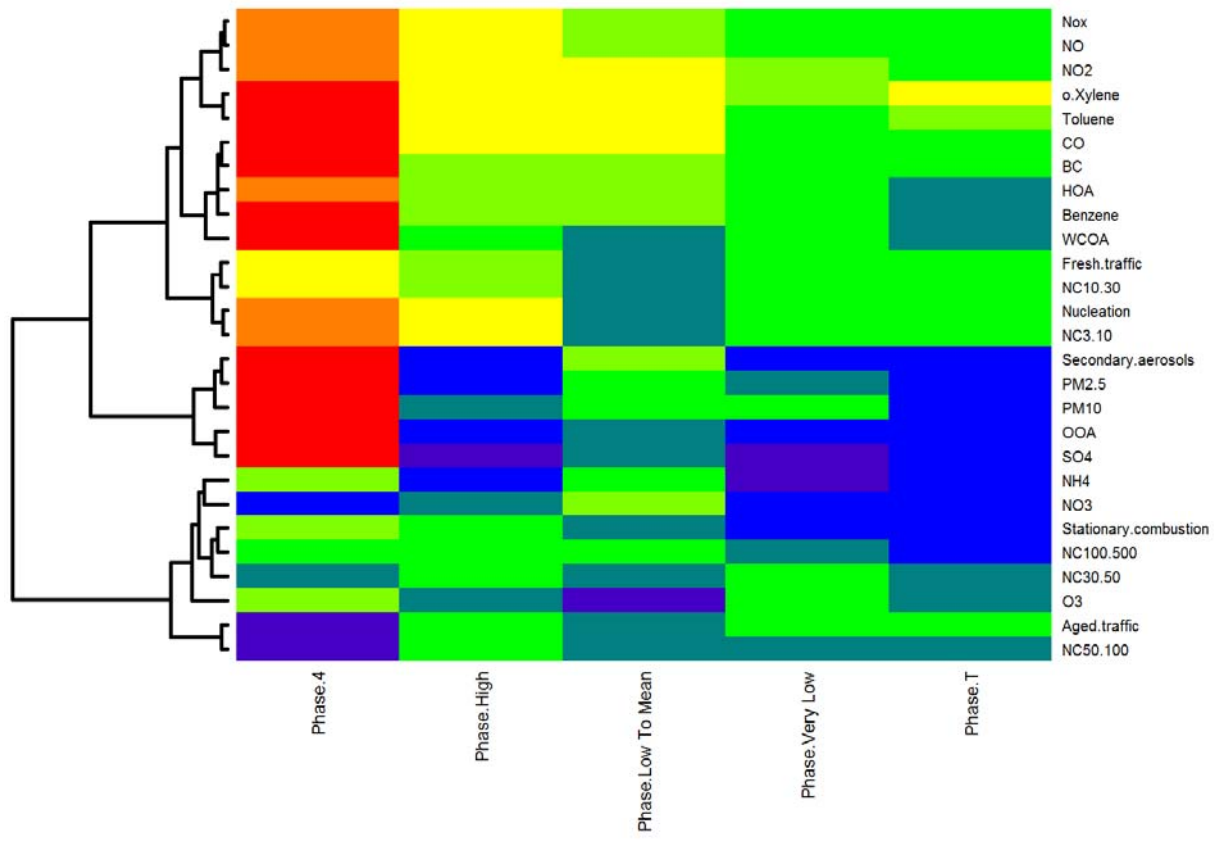


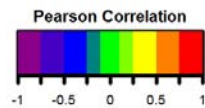
RH



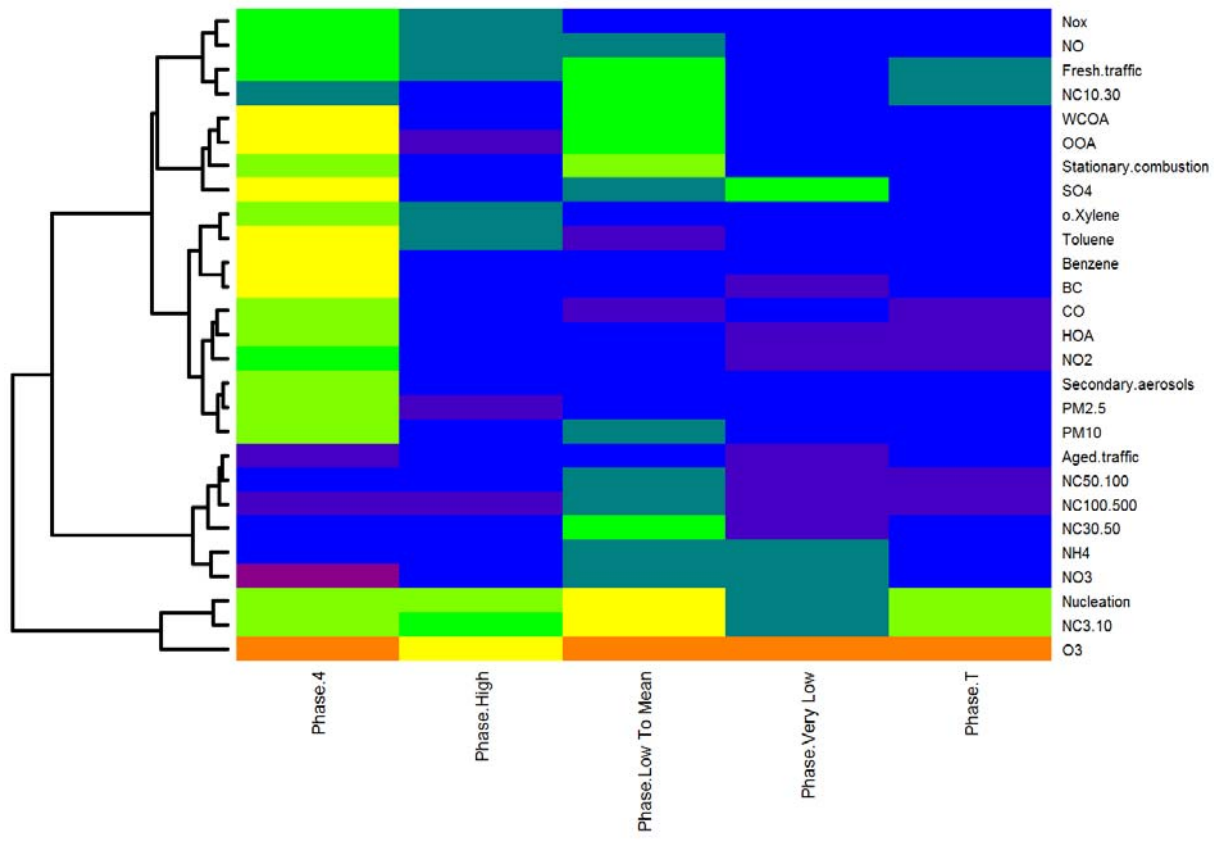


AH





WS



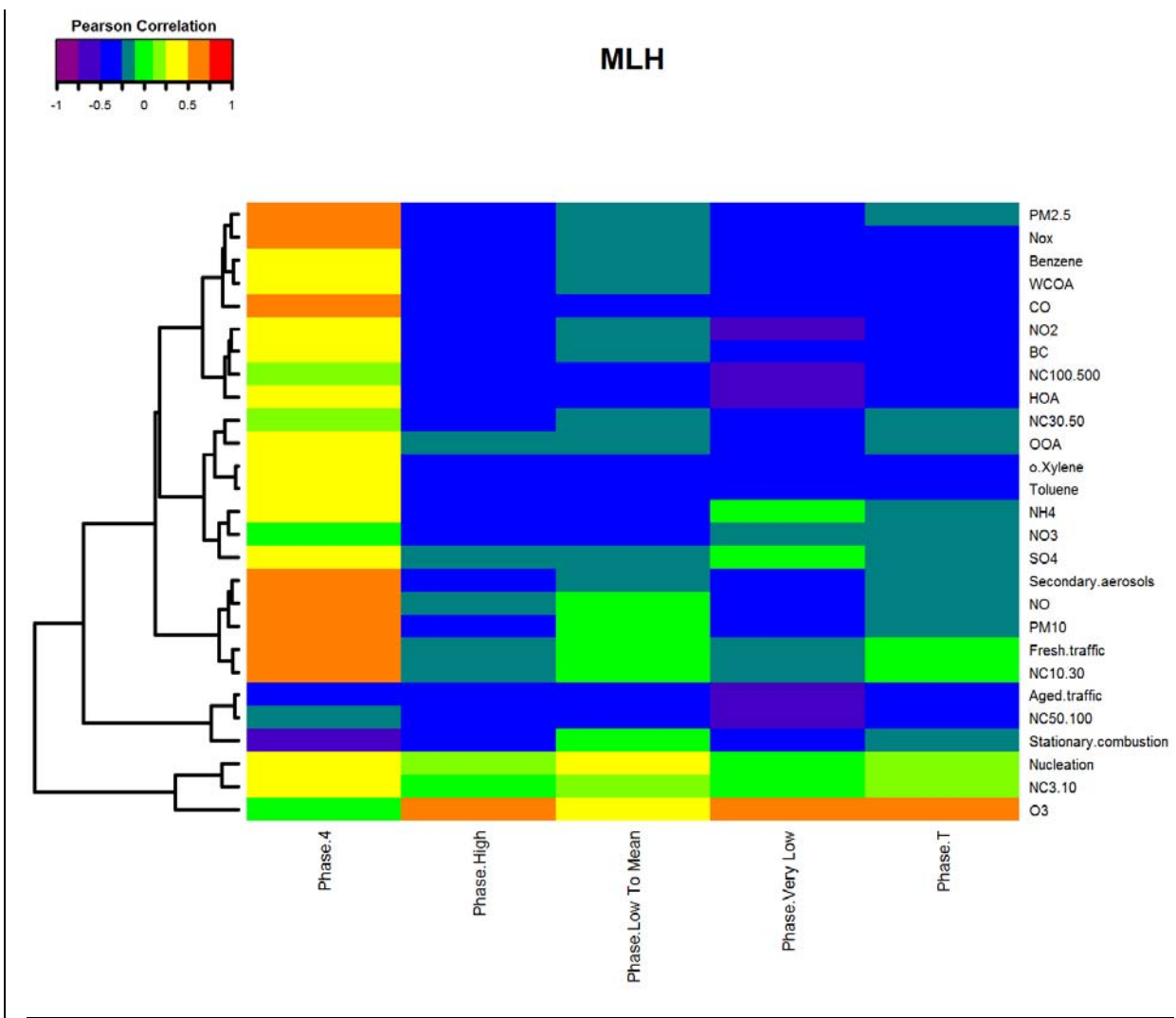
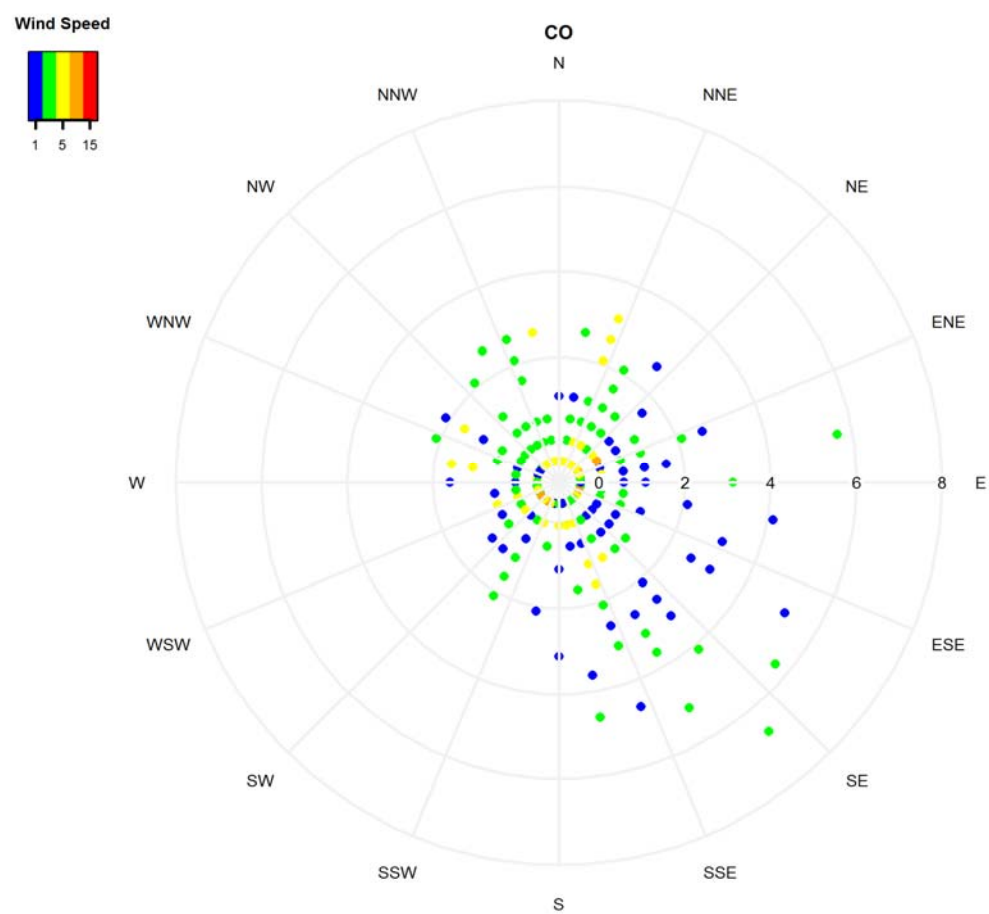


Figure 6. Heatmap with Pearson intercorrelations between pollutants and meteorological parameters (T (temperature), RH (relative humidity), AH (absolute humidity), WS (wind speed), MLH (mixing layer height)) during the measurement period for three groups (phases Very Low, Low To Mean and High concentrations), phase 4 and total period (phase Total) including the dendrogram on the rows. The correlations are coloured according to the scale on the top-left corner.



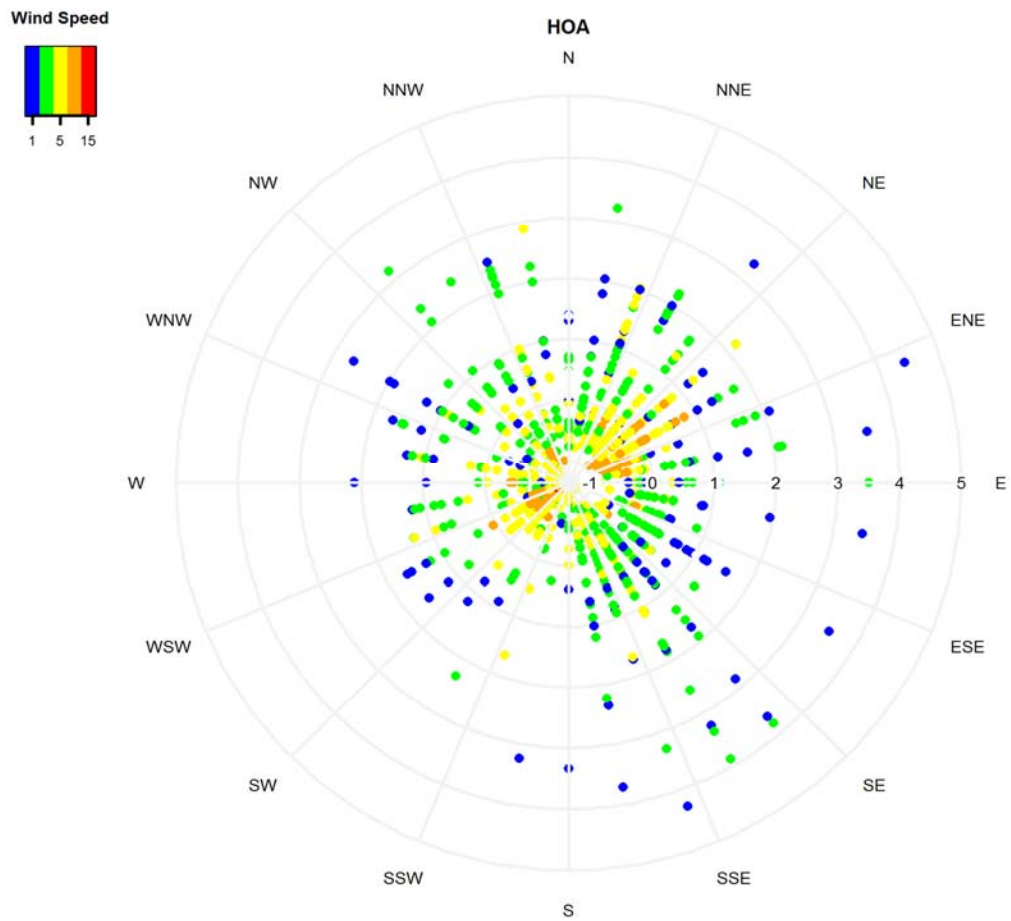


Figure 7. Wind direction, wind speed (in different colours, units in m/s) and concentration (in different distance to the middle, scale on the horizontal line in $\mu\text{g}/\text{m}^3$) plots in polar coordinates for CO and HOA - hydrocarbon-like organic aerosol. Calm wind situations are in blue. The correlations are coloured according to the scale on the top-left corner.

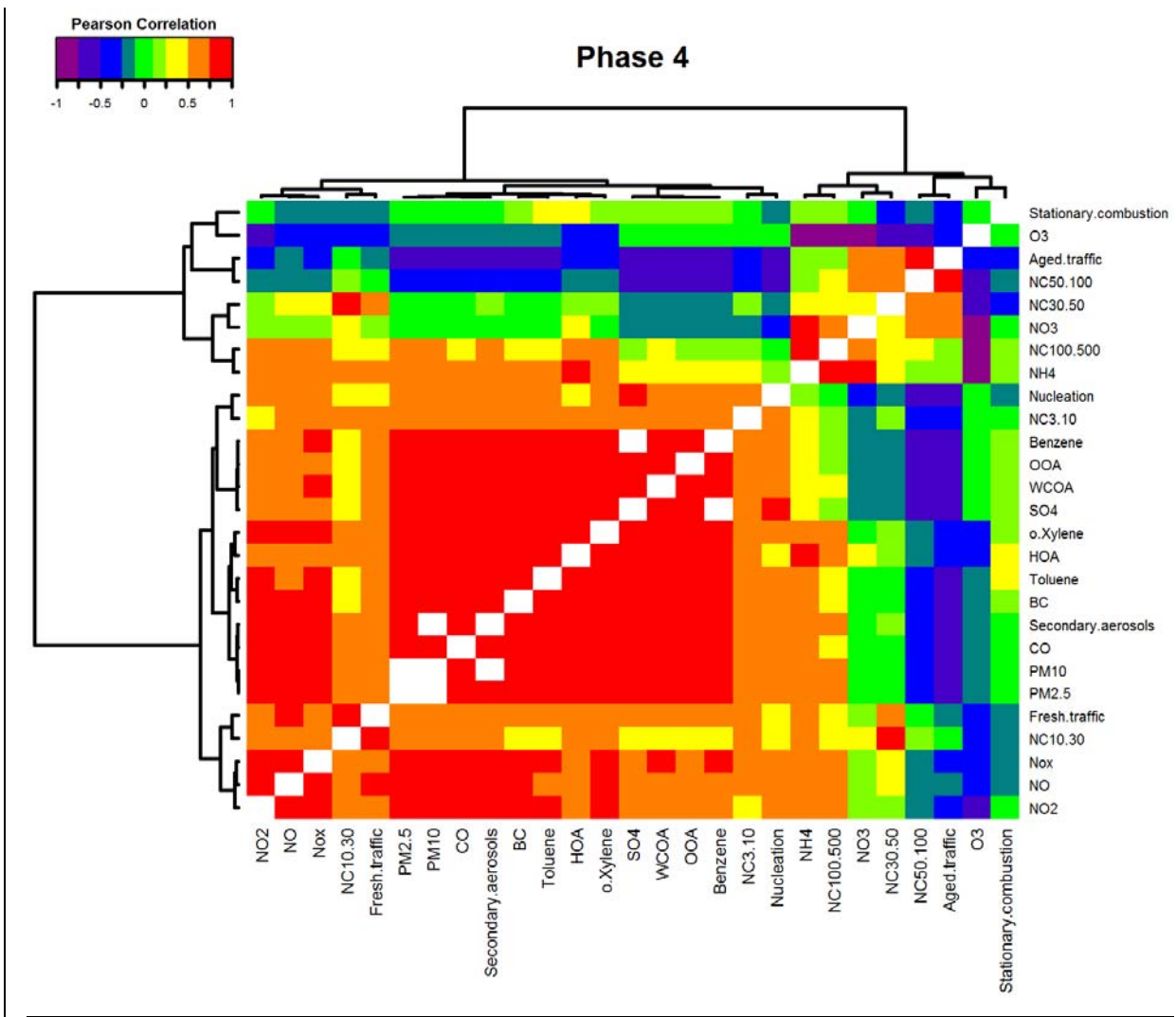
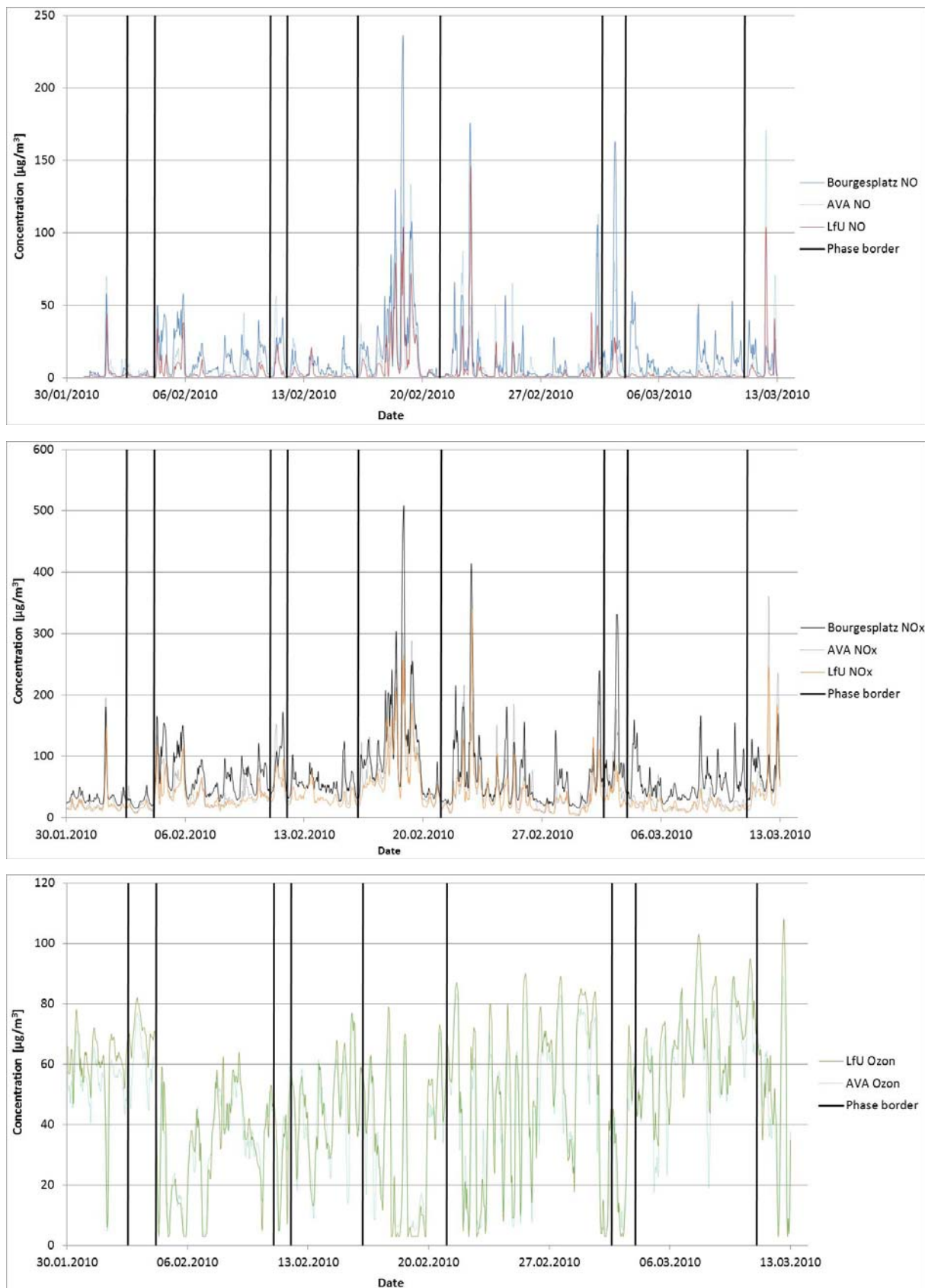


Figure 8. Heatmap with Pearson intercorrelations between all pollutants during phase 4 showing different clusters including the dendrogram on the rows and columns. The correlations are coloured according to the scale on the top-left corner.

Supplements:



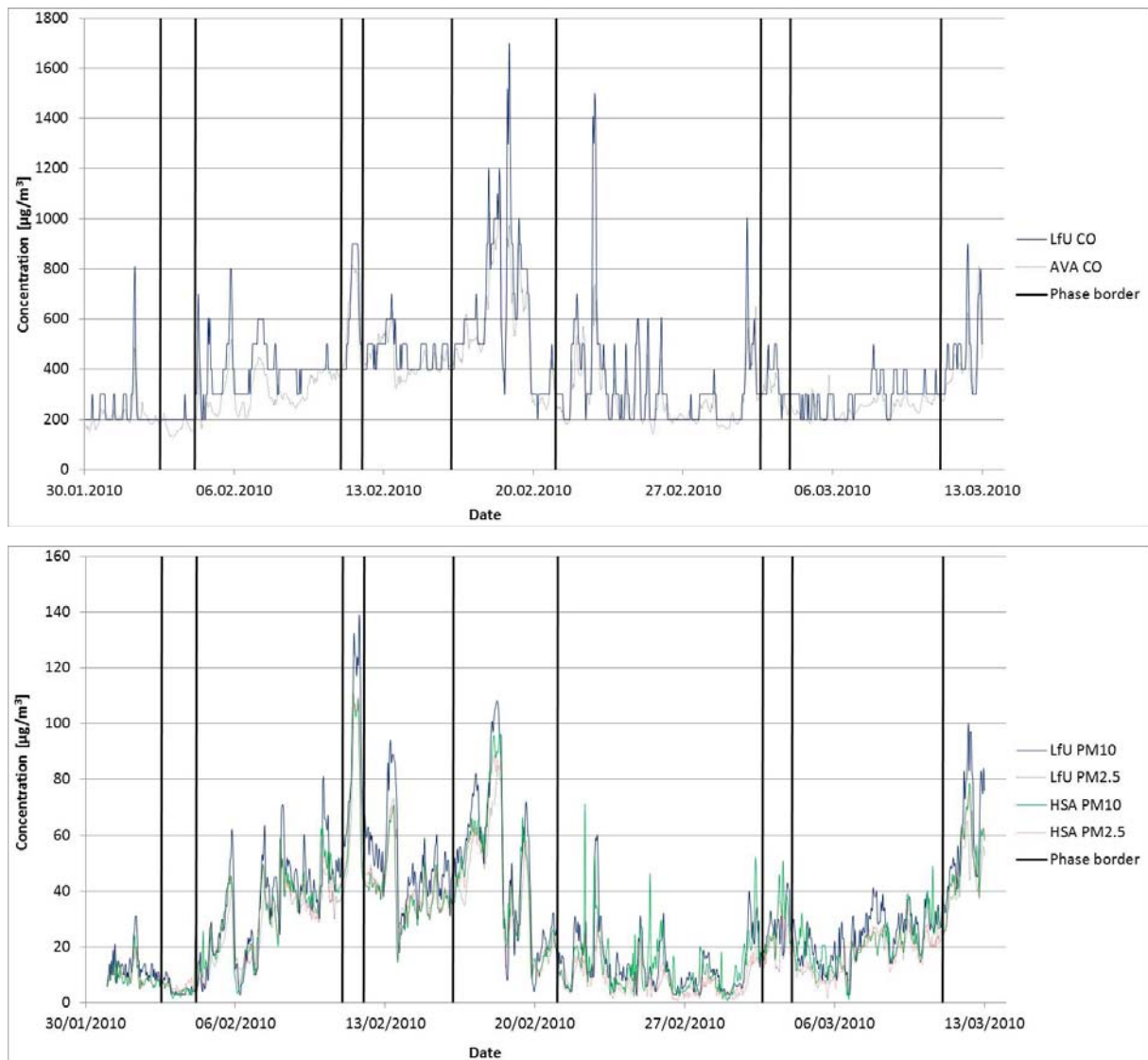
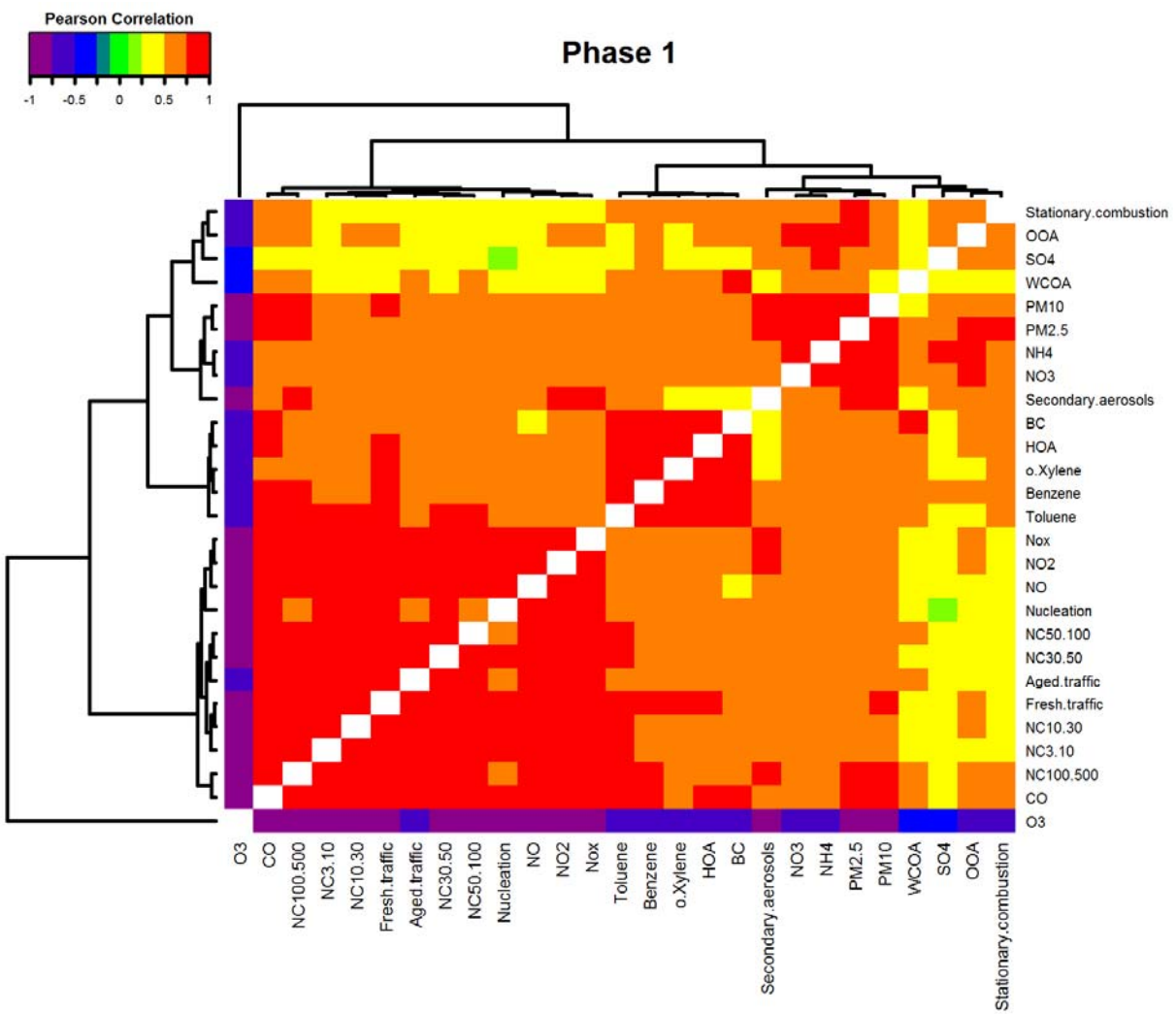
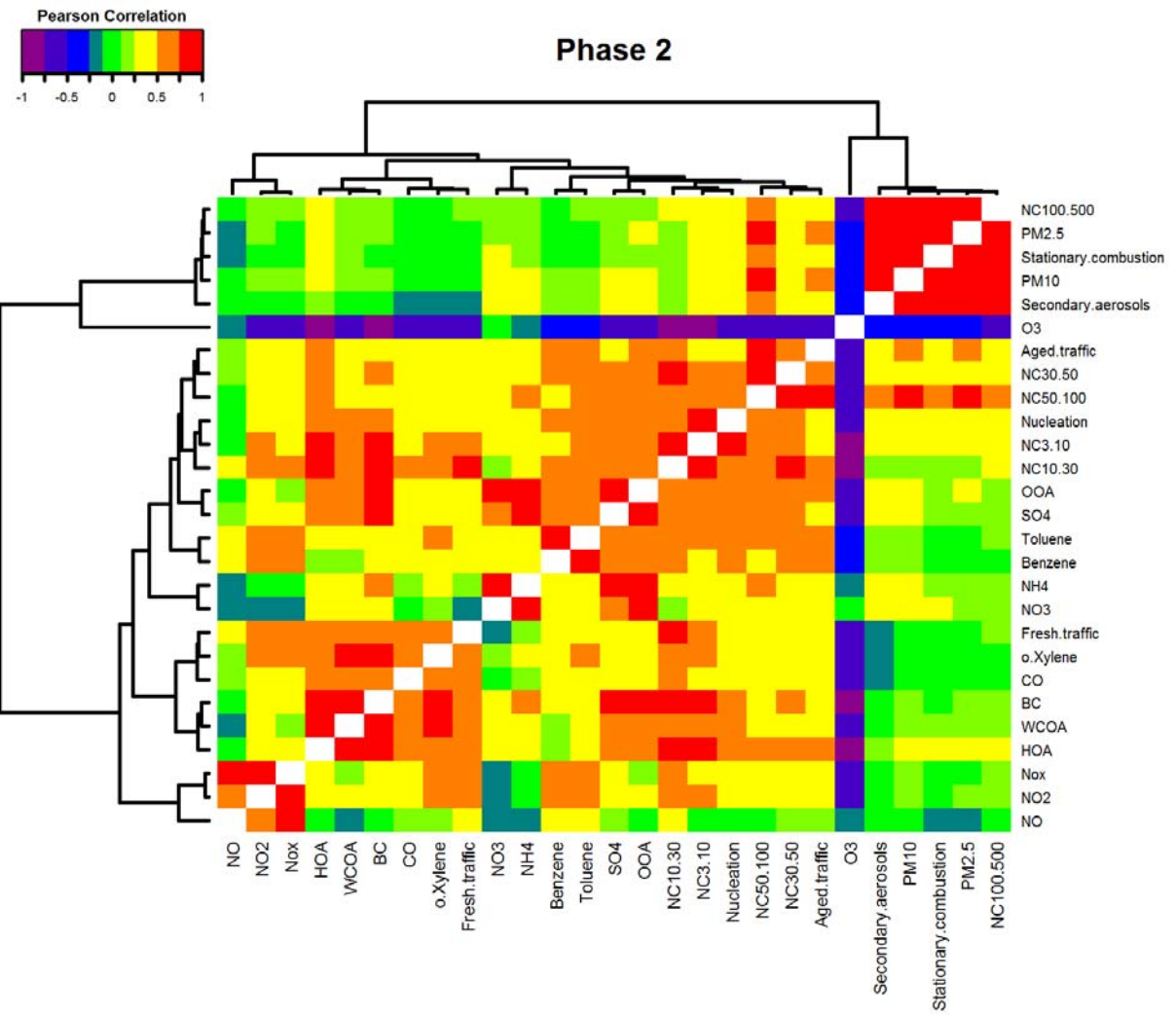
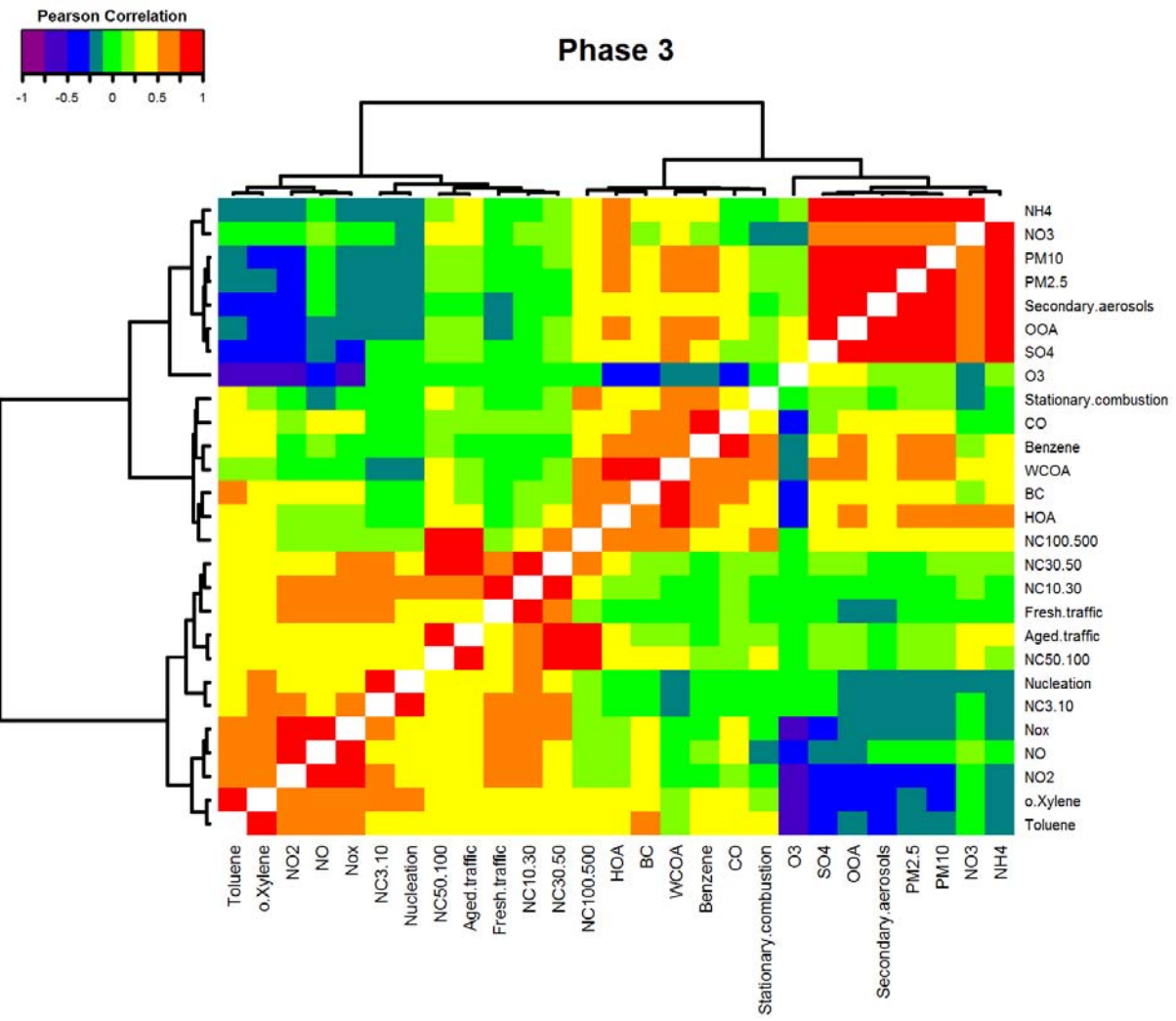
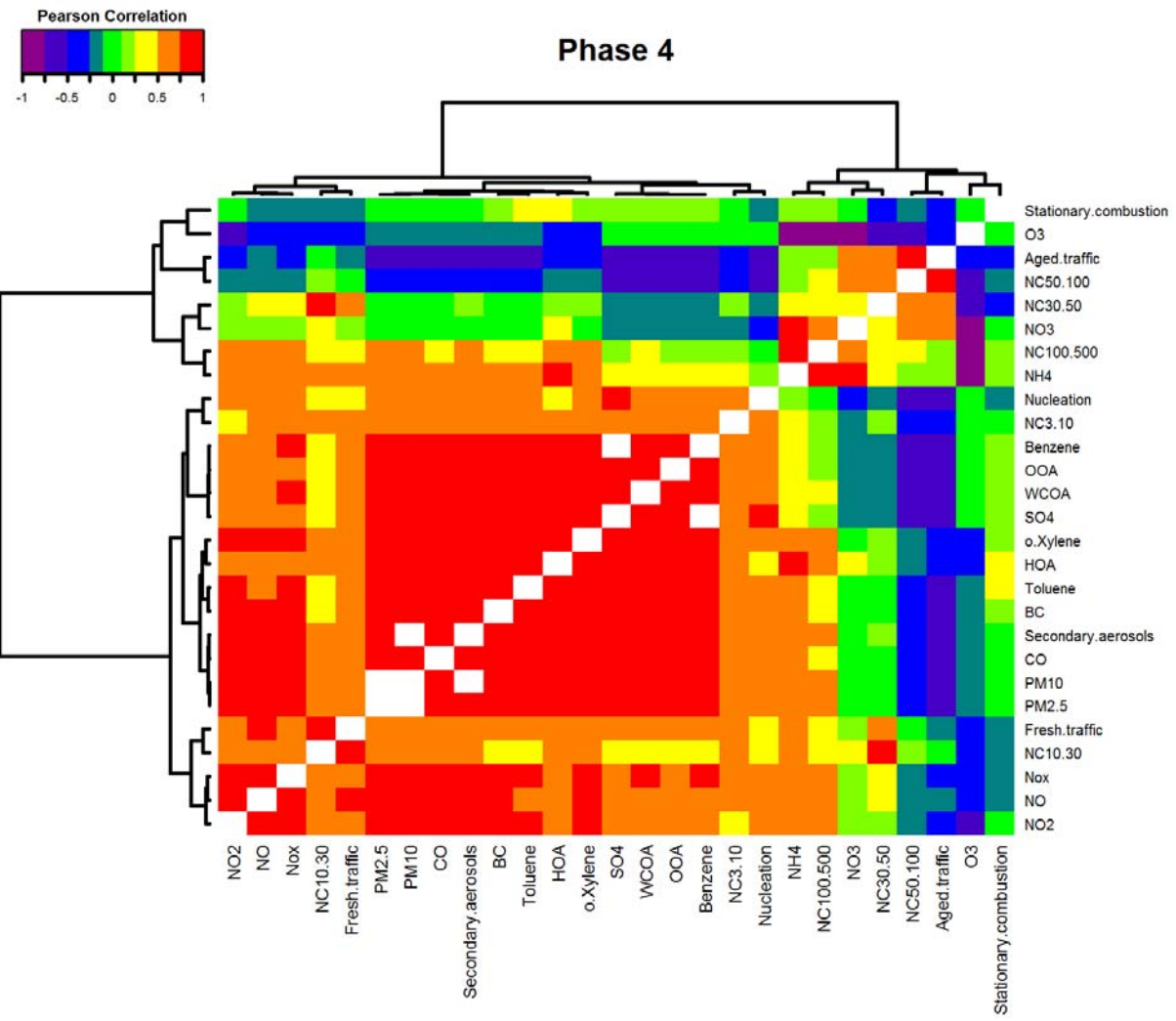


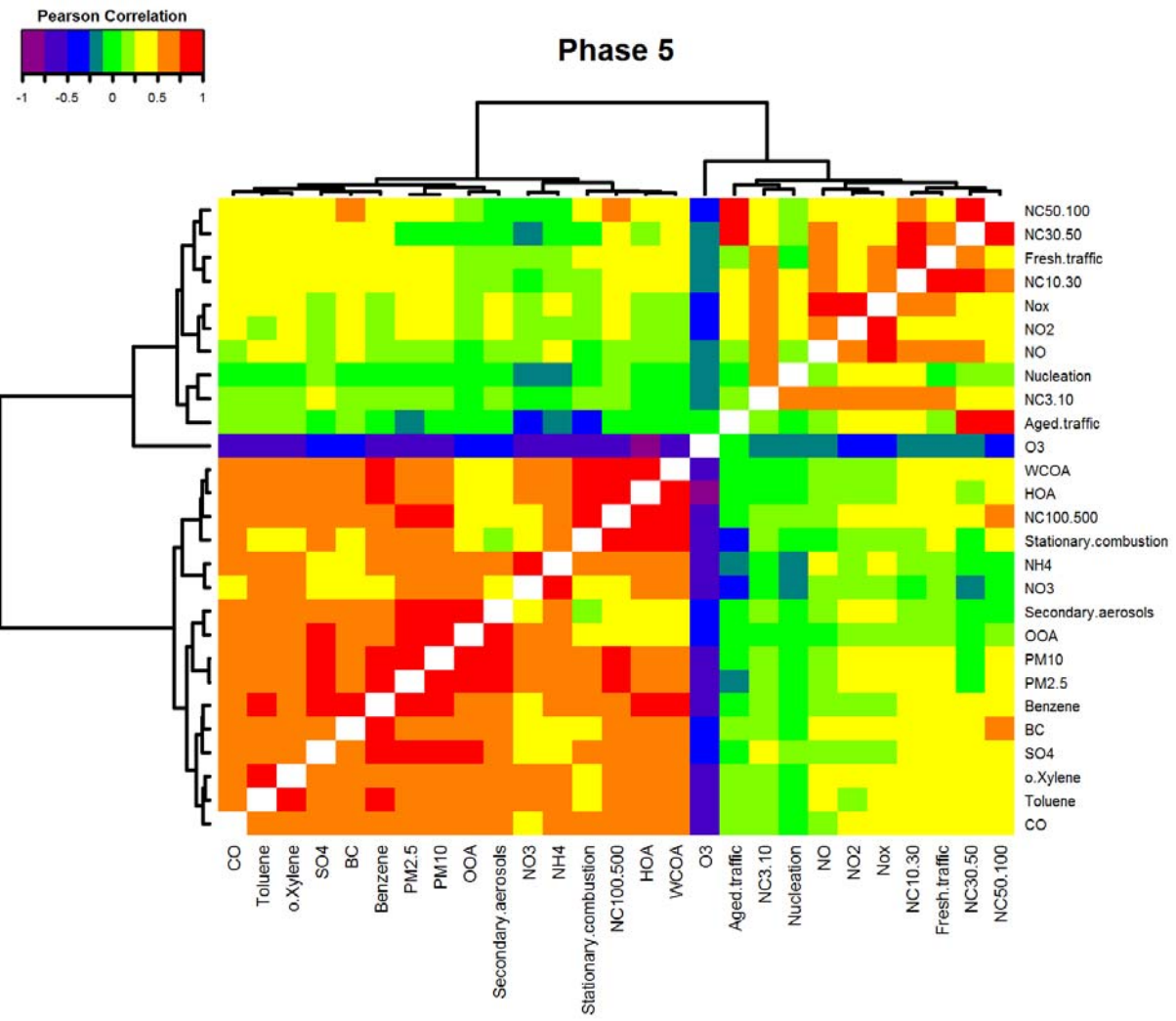
Figure S1: Measurement results of hourly-mean values NO, NO_x, O₃, CO, PM_{2.5} and PM₁₀ concentrations at the sites Bourgesplatz (LÜB), LfU (LÜB), HSA and AVA. The temporal resolutions of CO data at LfU and AVA are different due to the different measurement principles. The borders of the 10 phases are drawn too.

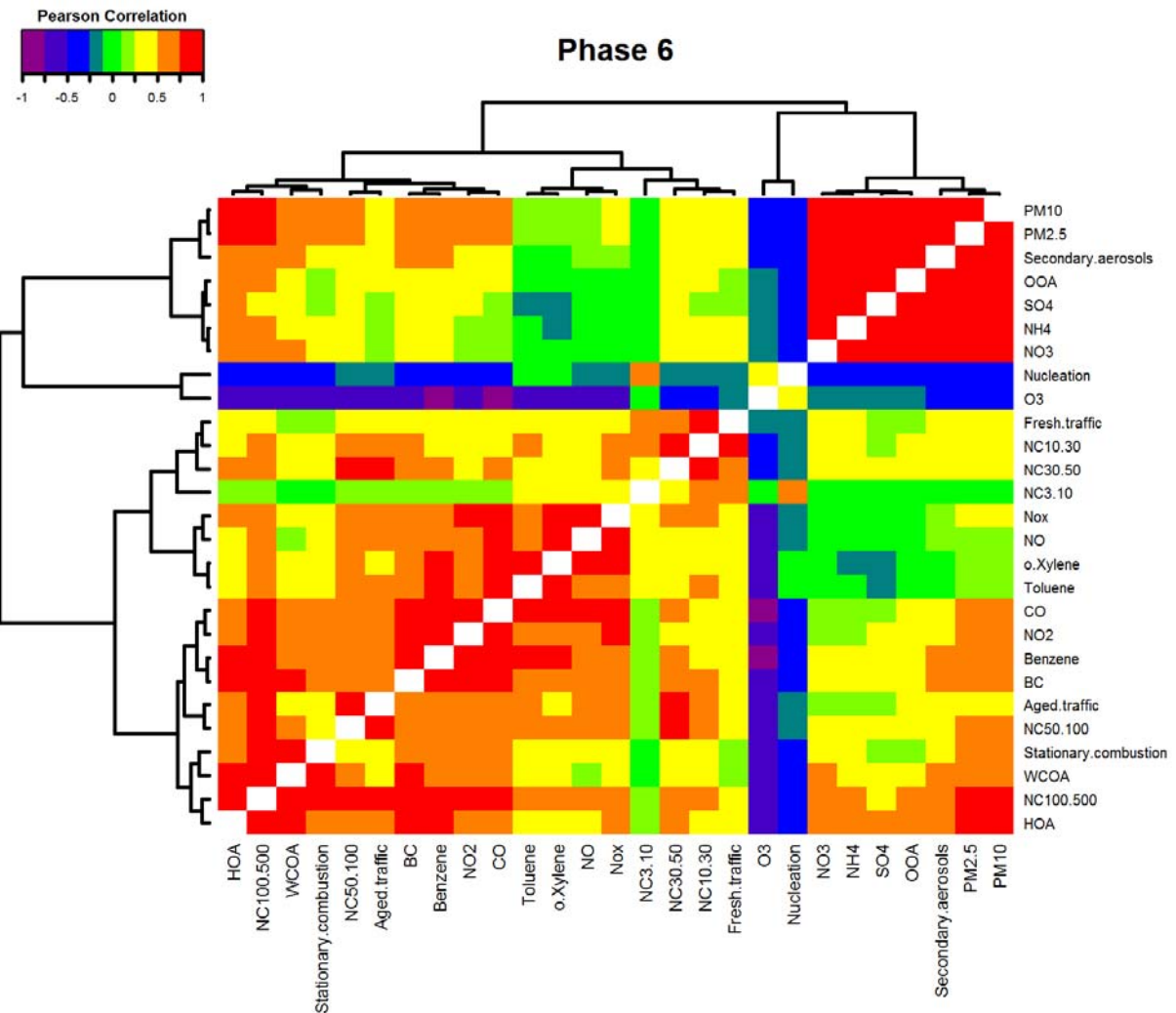


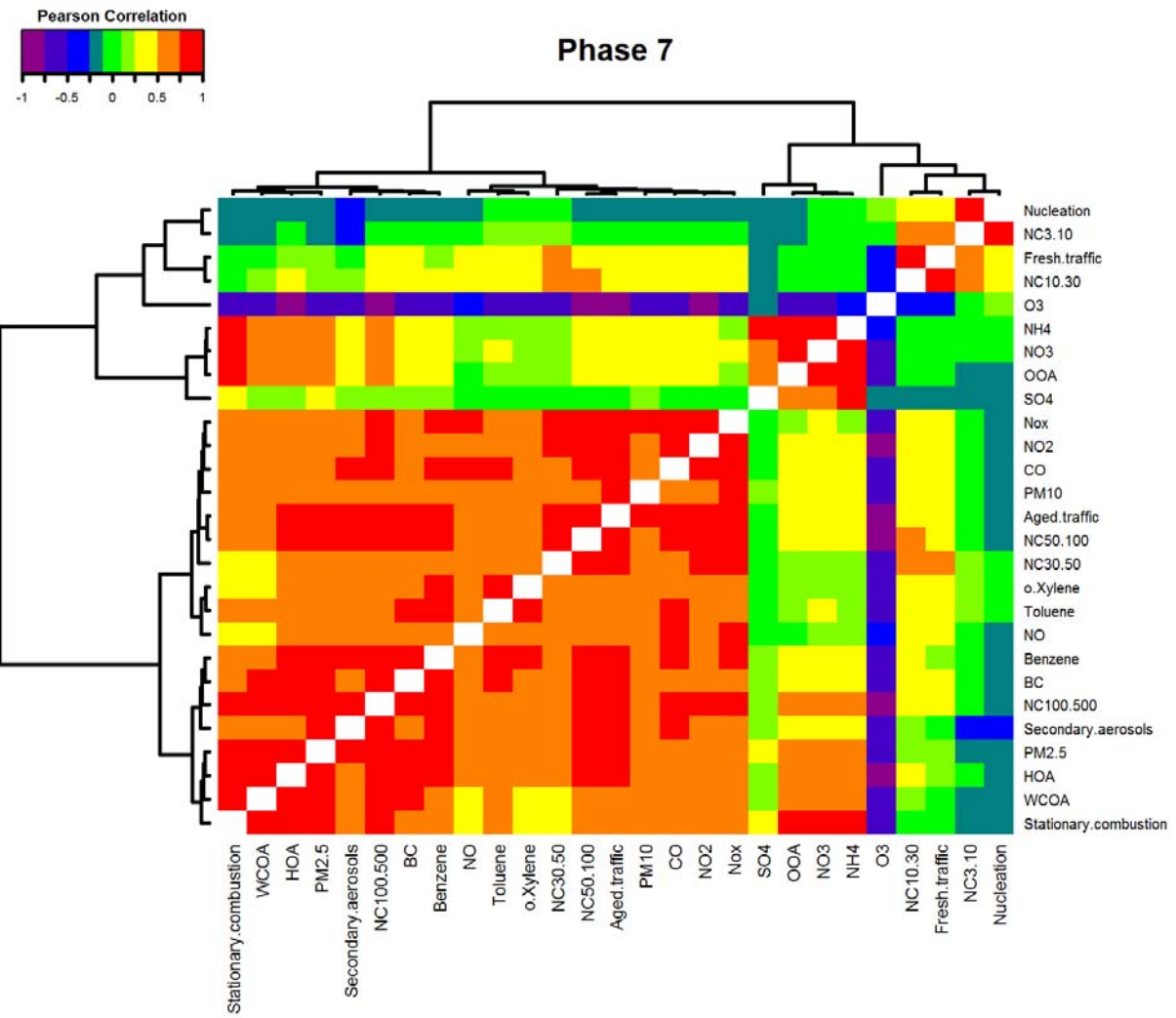


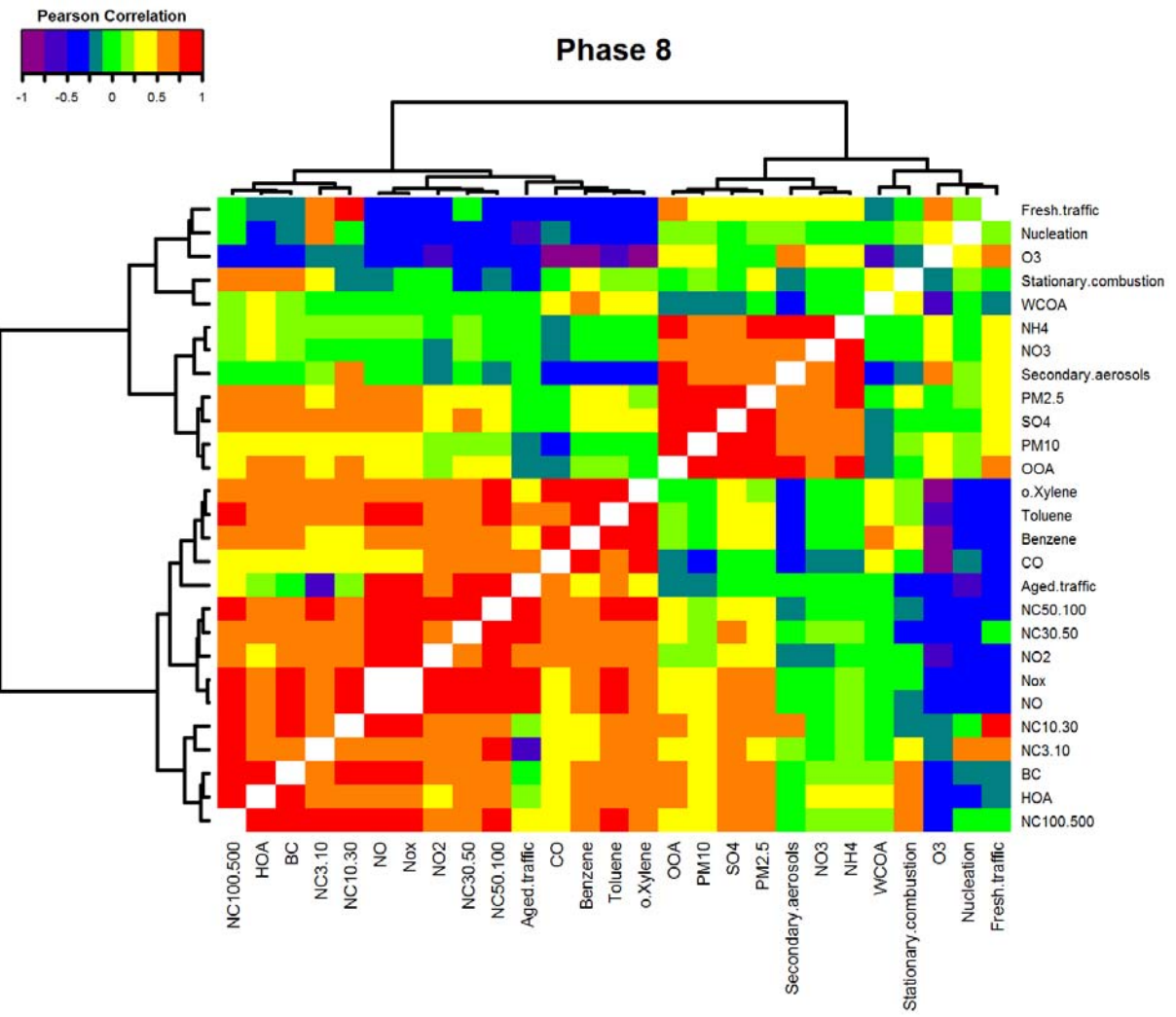


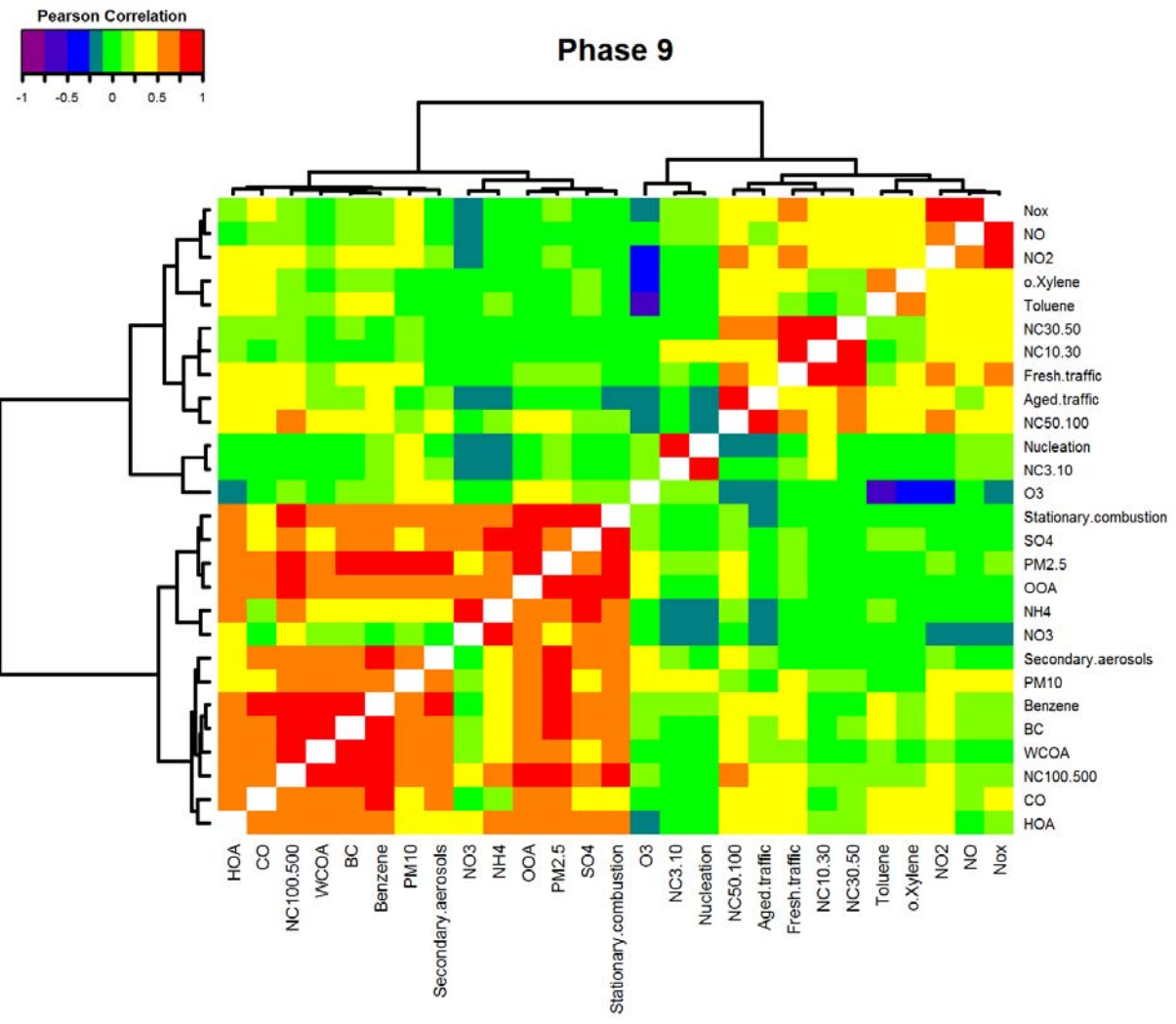












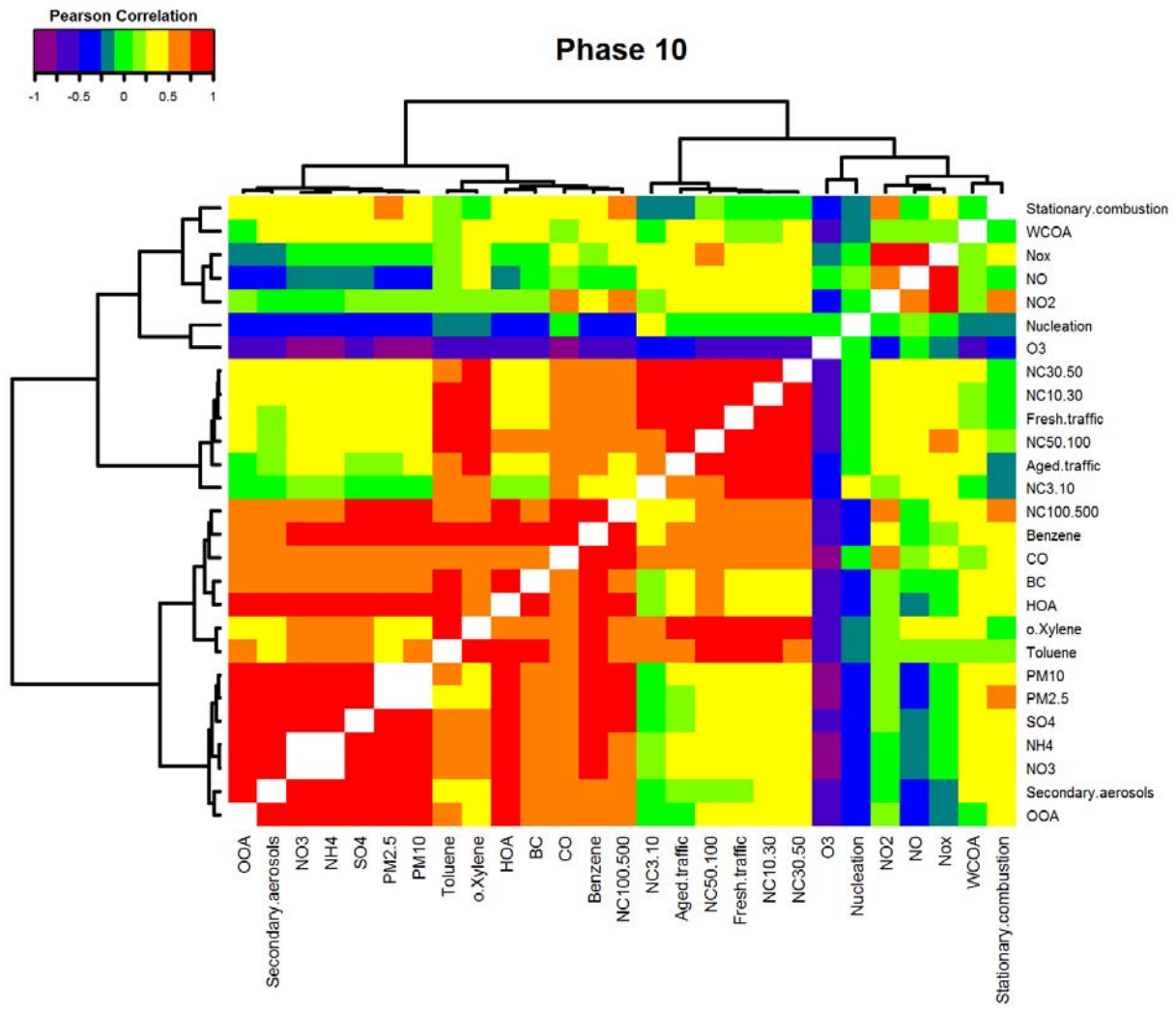


Figure S2: Heatmaps with Pearson intercorrelations between all pollutants during all 10 measurement periods showing different clusters including the two-dimensional dendrogram on the rows and columns (phase 4 is shown in Figure 4 also). The correlations are coloured according to the scale on the top-left corner. Correlations between the same variables (equal to 1) are shown in white.

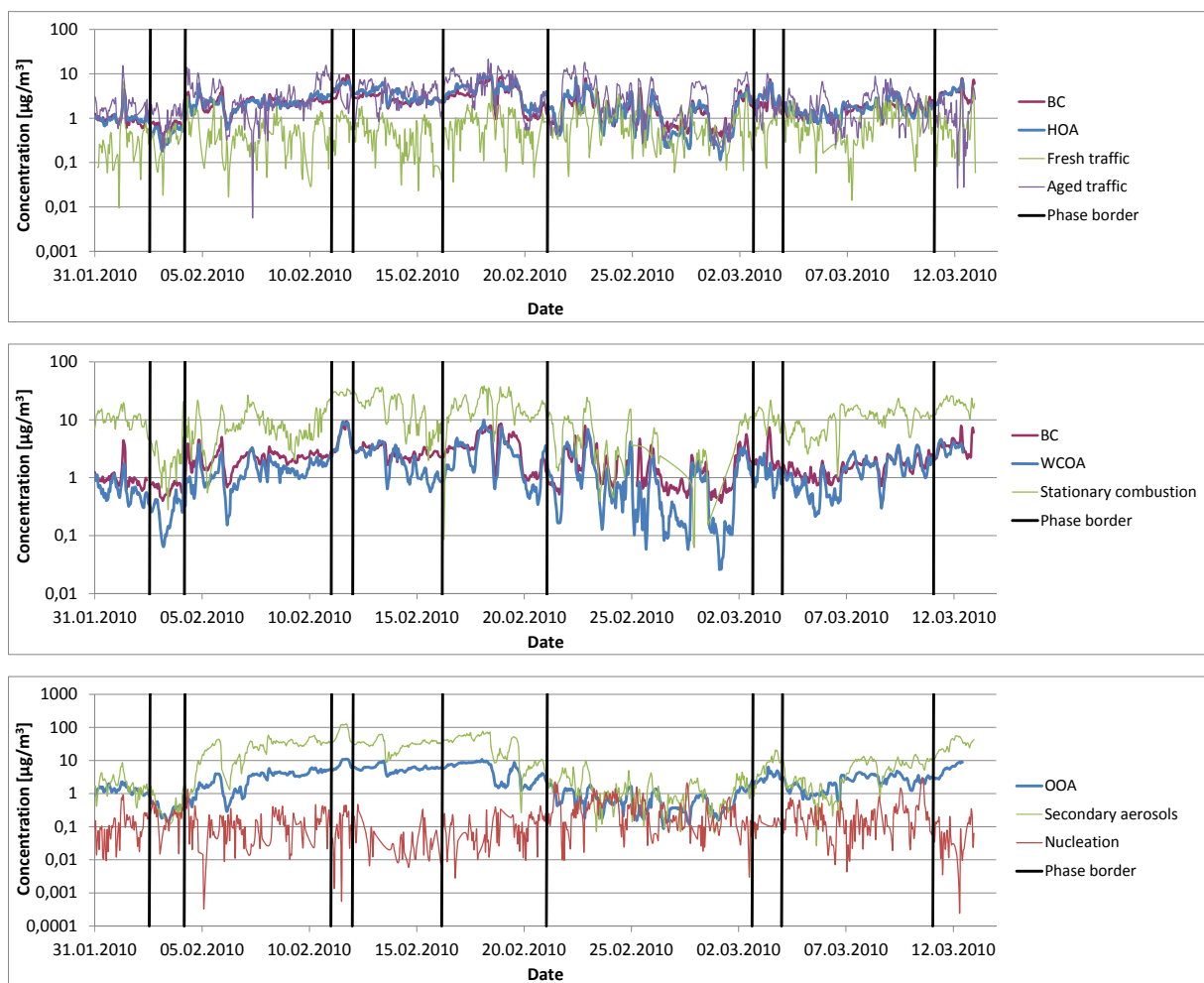


Figure S3: Comparison of the different factors from PMF analyses of PSD data in the size range from 3.8 nm to 800 nm with those from PMF analyses of PM_1 composition on the basis of hourly-mean values: fresh traffic and aged traffic aerosol factors with black carbon (BC) and hydrocarbon-like organic aerosol (HOA, traffic factor or primary organic factor), stationary combustion aerosol factor with black carbon (BC) and wood combustion organic aerosol (WCOA, wood combustion factor) as well as secondary aerosol factor with oxygenated organic aerosol (OOA, secondary organic factor) together with nucleation aerosol factor. The borders of the 10 phases are drawn too.

Table S1: Quantitative characterization of the 10 temporal phases from 31 January, 00:00 CET to 12 March 2010, 24:00 CET of PM components soot (BC - black carbon), OOA - oxygenated organic aerosol (secondary organic factor), HOA - hydrocarbon-like organic aerosol (traffic factor or primary organic factor), WCOA - wood combustion organic aerosol (wood combustion factor), nitrate (NO_3^-), sulphate (SO_4^{2-}) and ammonium (NH_4^+) (see text).

Phase	Description	mean [$\mu\text{g}/\text{m}^3$]			relative	Starting date in CET
1	Constant phase with relatively low PMC and higher NO_3^- content. Wind speeds from 1 to 9 m/s. Prevailing wind direction west-southwest. Temperatures from -9 to -3°C.	Organic Nitrate Sulphate Ammonium Soot	Total	3.21	0.30	31/01/2010 00:00
			OOA	1.32	0.12	
			HOA	1.10	0.10	
			WCOA	0.70	0.07	
				4.17	0.36	
				1.29	0.12	
				1.46	0.13	
2	Decrease to very low PMC. Soot and primary PMF factor HOA play the dominant role. Wind speeds from 6 to 14 m/s. Prevailing wind direction west-southwest. Temperatures from -3 to +3°C.	Organic Nitrate Sulphate Ammonium Soot	Total	1.15	0.36	02/02/2010 13:00
			OOA	0.37	0.11	
			HOA	0.48	0.16	
			WCOA	0.28	0.09	
					0.20	
				0.34	0.11	
				0.38	0.11	
3	Increase of PMC with mean composition, some less organic components. Wind speeds from 1 to 5 m/s. Varying wind directions from northwest to east. Temperatures from -8 to +7°C.	Organic Nitrate Sulphate Ammonium Soot	Total	6.72	0.31	04/02/2010 04:00
			OOA	3.00	0.13	
			HOA	2.26	0.11	
			WCOA	1.40	0.07	
					0.30	
				3.73	0.15	
				2.60	0.12	
4	Special event with strong PMC	Organic	Total	18.23	0.36	11/02/2010

	increase during "wet" snow fall. Higher SO_4^{2-} and WCOA contents. High CO, NO and NO_x concentrations. Wind speeds from 0.5 to 5 m/s. Wind directions west-northwest and north-northwest. Temperatures from -9 to -4°C.		OOA	7.99	0.15	00:00
			HOA	5.29	0.10	
			WCOA	5.53	0.10	
		Nitrate			0.24	
		Sulphate		10.05	0.20	
		Ammonium		5.08	0.10	
		Soot		5.35	0.10	
5	Steady high PMC with much SO_4^{2-} and OOA (secondary). Daily variations. Wind speeds from 0.5 to 3 m/s. Prevailing wind direction southeast. Temperatures from -7 to -3°C.	Organic	Total	11.22	0.34	12/02/2010 00:00
			OOA	5.84	0.18	
			HOA	3.41	0.10	
			WCOA	2.11	0.06	
		Nitrate			0.26	
		Sulphate			0.20	
		Ammonium			0.11	
		Soot			0.09	
6	Further PMC increase with high NO_3^- content. Highest CO, NO and NO_x concentrations. HOA (primary) and OOA (secondary) contents similar. Wind speeds from 0.5 to 7 m/s. Varying wind directions from north-northeast via east and south to west. Temperatures from -8 to +7°C.	Organic	Total	12.91	0.34	16/02/2010 04:00
			OOA	5.51	0.14	
			HOA	4.51	0.13	
			WCOA	2.84	0.07	
		Nitrate			0.35	
		Sulphate			0.09	
		Ammonium			0.11	
		Soot			0.10	
7	Strong PMC decrease. Main content is organic origin with HOA. WCOA and soot (BC) contents high. Some peak CO, NO and NO_x concentrations. Wind speeds from 1 to 13 m/s. Varying wind directions from south-southeast to west-southwest. Temperatures from -3 to	Organic	Total	3.48	0.46	21/02/2010 01:00
			OOA	0.72	0.12	
			HOA	1.62	0.22	
			WCOA	1.09	0.13	
		Nitrate			0.15	
		Sulphate			0.06	

	+13°C.	Ammonium			0.07		
		Soot			0.26		
8	Second special event with high PMC increase and high NO_3^- content during "wet" snow fall. Some peak CO, NO and NO_x concentrations. Wind speeds from 0 to 6 m/s. Prevailing wind direction east-northeast. Temperatures from -3 to +4°C.	Organic	Total	7.85	0.29	02/03/2010	
			OOA	3.23	0.12	15:00	
			HOA	3.14	0.12		
			WCOA	1.24	0.05		
			Nitrate		0.39		
		Sulphate			0.11		
			Ammonium		0.12		
			Soot		0.09		
		Organic	Total	5.48	0.36	04/03/2010	
			OOA	2.41	0.15	00:00	
9	Phase with low up to mean PMC. Mean composition with a little bit more WCOA. Wind speeds from 1 to 11 m/s. Wind directions northeast to east northeast and west-southwest. Temperatures from -12 to +4°C.		HOA	1.65	0.11		
			WCOA	1.36	0.09		
	Nitrate			0.27			
		Sulphate		0.16			
		Ammonium		0.11			
	Soot			0.11			
10	PMC increase with more WCOA. Wind speeds from 0 to 4 m/s. Varying wind directions from west southwest to north northeast. Temperatures from -12 to +2°C.	Organic	Total	12.61	0.36	11/03/2010	
			OOA	5.59	0.15	01:00	
			HOA	3.79	0.11		
			WCOA	3.23	0.10		
			Nitrate		0.30		
		Sulphate			0.13		
			Ammonium	4.27	0.11		
			Soot	3.76	0.11		

Table S2: Pearson correlation coefficients between all pollutants during the total measurement period (all temporal phases) on the basis of hourly-mean values. Correlation coefficients > 0.8 are in bold, and correlations, which are not significant (p -value >0.05), are in italics

Phase.Total	CO	O3	NO	NO2	NOx	Benzene	Toluene	o.Xylene	PM2.5	PM10	BC	NO3	SO4	NH4	OOA	HOA	WCOA	NC3.10	NC10.30	NC30.50	NC50.100	NC100.500	Nucleation	Fresh.traffic	Aged.traffic	Statiory.combustion	Secondary.aerosols
CO	1																										
O3	-0.67	1																									
NO	0.64	-0.43	1																								
NO2	0.78	-0.66	0.69	1																							
NOx	0.75	-0.57	0.95	0.88	1																						
Benzene	0.89	-0.57	0.47	0.63	0.58	1																					
Toluene	0.75	-0.59	0.65	0.66	0.71	0.67	1																				
o.Xylene	0.64	-0.51	0.62	0.63	0.68	0.53	0.90	1																			
PM2.5	0.67	-0.41	0.24	0.43	0.34	0.82	0.29	0.14	1																		
PM10	0.70	-0.42	0.32	0.51	0.42	0.82	0.35	0.22	0.97	1																	
BC	0.83	-0.58	0.52	0.68	0.63	0.91	0.68	0.56	0.79	0.81	1																
NO3	0.49	-0.40	0.17	0.31	0.25	0.57	0.21	0.09	0.79	0.77	0.57	1															
SO4	0.42	-0.20	<i>0.04</i>	0.17	0.10	0.64	<i>0.06</i>	-0.08	0.88	0.83	0.56	0.68	1														
NH4	0.50	-0.35	0.14	0.28	0.21	0.63	0.16	0.03	0.88	0.84	0.60	0.97	0.84	1													
OOA	0.56	-0.26	0.12	0.32	0.22	0.73	0.17	0.02	0.93	0.90	0.68	0.82	0.90	0.91	1												
HOA	0.79	-0.61	0.44	0.66	0.57	0.84	0.57	0.45	0.81	0.82	0.90	0.74	0.61	0.74	0.76	1											
WCOA	0.70	-0.49	0.27	0.53	0.40	0.81	0.46	0.33	0.77	0.76	0.85	0.56	0.57	0.59	0.66	0.85	1										
NC3.10	-0.04	0.08	0.19	0.09	0.16	-0.09	0.13	0.17	-0.14	-0.07	-0.02	-0.16	-0.16	-0.17	-0.15	-0.07	-0.07	1									
NC10.30	0.24	-0.20	0.48	0.40	0.48	0.15	0.37	0.39	0.08	0.17	0.28	0.10	0.01	0.07	0.05	0.24	0.11	0.55	1								
NC30.50	0.51	-0.39	0.53	0.60	0.60	0.41	0.51	0.48	0.28	0.36	0.47	0.27	0.16	0.24	0.24	0.47	0.34	0.22	0.77	1							
NC50.100	0.70	-0.57	0.59	0.74	0.70	0.61	0.61	0.54	0.45	0.50	0.64	0.39	0.29	0.38	0.40	0.67	0.53	0.11	0.51	0.83	1						
NC100.500	0.80	-0.58	0.45	0.65	0.57	0.85	0.53	0.40	0.82	0.81	0.83	0.66	0.66	0.70	0.74	0.88	0.81	-0.05	0.24	0.53	0.79	1					
Nucleation	-0.17	0.20	-0.03	-0.06	-0.05	-0.20	0.01	0.06	-0.26	-0.20	-0.17	-0.28	-0.25	-0.29	-0.26	-0.23	-0.16	0.90	0.36	0.01	-0.11	-0.21	1				
Fresh.traffic	0.26	-0.19	0.37	0.41	0.41	0.16	0.38	0.42	0.07	0.15	0.23	0.08	-0.02	0.05	0.03	0.20	0.11	0.43	0.94	0.69	0.43	0.19	0.22	1			
Aged.traffic	0.62	-0.54	0.56	0.70	0.66	0.49	0.57	0.54	0.29	0.36	0.51	0.25	0.13	0.22	0.24	0.53	0.37	0.01	0.50	0.82	0.94	0.64	-0.11	0.35	1		
Statiory.combustion	0.60	-0.37	0.24	0.39	0.32	0.70	0.32	0.19	0.72	0.67	0.67	0.61	0.63	0.66	0.68	0.74	0.76	-0.13	0.06	0.25	0.47	0.85	-0.22	0.04	0.23	1	
Secondary.aerosols	0.61	-0.36	0.18	0.35	0.27	0.76	0.23	0.08	0.96	0.92	0.71	0.73	0.87	0.83	0.89	0.71	0.67	-0.16	0.05	0.24	0.36	0.71	-0.24	0.02	0.25	0.56	1

Table S3: Pearson correlation coefficient of each pollutant with each meteorological parameter (T (temperature), RH (relative humidity), AH (absolute humidity), WS (wind speed), MLH (mixing layer height)) during the total measurement period on the basis of hourly-mean values. Bold values are values, which are not lower than 33 % of the maximum value, and italic values are those which are not significant (p-value >0.05).

Phase.Total	T	RH	AH	WS	MLH
CO	-0.27	0.43	-0.02	-0.52	-0.33
O3	0.18	-0.62	-0.22	0.64	0.55
NO	<i>0.00</i>	0.17	0.10	-0.25	-0.17
NO2	-0.11	0.30	0.09	-0.53	-0.37
Nox	<i>-0.05</i>	0.23	0.10	-0.39	-0.26
Benzene	-0.40	0.45	-0.15	-0.49	-0.28
Toluene	<i>0.03</i>	0.27	0.22	-0.39	-0.31
o.Xylene	0.14	0.17	0.29	-0.30	-0.29
PM2.5	-0.55	0.48	-0.31	-0.45	-0.19
PM10	-0.48	0.40	-0.29	-0.44	-0.17
BC	-0.30	0.41	-0.05	-0.48	-0.31
NO3	-0.49	0.43	-0.27	-0.40	-0.22
SO4	-0.65	0.40	-0.47	-0.35	-0.11
NH4	-0.59	0.45	-0.37	-0.40	-0.19
OOA	-0.60	0.39	-0.41	-0.41	-0.14
HOA	-0.39	0.47	-0.12	-0.56	-0.37
WCOA	-0.39	0.38	-0.18	-0.39	-0.27
NC3.10	0.20	-0.31	<i>0.00</i>	0.14	0.16
NC10.30	<i>0.02</i>	-0.08	<i>-0.03</i>	-0.16	-0.08
NC30.50	-0.17	0.08	-0.12	-0.34	-0.23
NC50.100	-0.32	0.27	-0.16	-0.50	-0.37
NC100.500	-0.51	0.46	-0.26	-0.53	-0.34
Nucleation	0.31	-0.41	0.04	0.23	0.24
Fresh.traffic	<i>0.03</i>	<i>-0.05</i>	<i>0.02</i>	-0.16	<i>-0.07</i>
Aged.traffic	-0.19	0.18	-0.07	-0.45	-0.36
Stationary.combustion	-0.55	0.43	-0.32	-0.35	-0.23
Secondary.aerosols	-0.49	0.43	-0.28	-0.41	-0.14